that the majority of cases showed activation of canonical NF-κB pathways through overexpression of p50, whereas only about 27% also concurrently engaged the non-canonical pathway. Our study therefore provides further evidence for the importance of NF-κB in NKTL, in line with the recent report by Huang *et al* [11].

Mutations of p53 resulting in overexpression of the protein have been demonstrated in a significant proportion of NKTLs [4,34]. Our data are not only consistent with these previous studies but further suggest that p53 deregulation is very common in NKTL. While abnormalities in p53 and NF-κB signalling have been reported in NKTL, Myc activation has not been previously described. The deregulation of these pathways in NKTL may explain the aggressive behaviour and relative drug resistance of these tumours [8,28]. It may also explain the efficacy of Velcade, which acts partly through targeting the NF-κB pathway [35].

While deregulation of p53 by mutations is described in NKTL, events mediating the activation of NF-κB and Myc pathways are unknown. We did not find any rearrangements in the *MYC* locus by FISH, suggesting that the activation of Myc in NKTL may be via *trans* mechanisms. A search of published data on NKTL revealed that abnormalities of DNA regions containing the genomic loci of the different NF-κB genes have not been described, indicating that the activation of NF-κB in NKTL is unlikely to be attributed to chromosomal alterations [10]. It may be possible that the constitutive activation of this pathway is the result of mutations in the NF-κB pathways, as was recently reported in lymphomas and myelomas [36,37].

As c-Myc is a transcriptional target of the EBV proteins EBNA2 [38] and LMP1 [39], and LMP1 is essential for EBV-mediated lymphocyte transformation by aggregating cellular proteins of the tumour necrosis factor receptor signalling pathway to activate NF-κB [40], it is possible that the activation of Myc and NF-κB in NKTL could be through the activity of EBV-related protein. This would be consistent with the importance of EBV infection in the pathogenesis of NKTL. Indeed, in EBV-immortalized B cells showing a latency III pattern, c-Myc and NF-κB are the two main transcriptional systems that are activated [41]. It is interesting to postulate that since EBV in NKTL shows a latency II pattern and lacks expression of EBNA-2 [2,3], the activation of c-Myc and NF-κB may be mediated primarily through LMP-1.

In this study, we observed remarkable overexpression of survivin in 97% of the NKTL samples. Survivin belongs to a family of human inhibitors of apoptosis and functions to counteract cell death by inhibiting caspase-9 activity and the intrinsic pathway of apoptosis [42]. Overexpression of survivin has been reported in many cancers, including some lymphomas, but has not been described in NKTL. In lymphomas, overexpression of survivin is associated with aggressive subtypes and inferior outcome [42,43]. Survivin is one of the target genes of NF-κB [30]. In addition, p53 deregulation can also contribute to the up-regulation of survivin, as demonstrated in melanoma [44], acute lymphoblastic leukaemia, and hepatocellular carcinoma. Therefore, the almost universal expression of survivin in NKTL is possibly downstream of p53 deregulation and/or NF-κB activation, which was observed in almost all of our cases of NKTL.

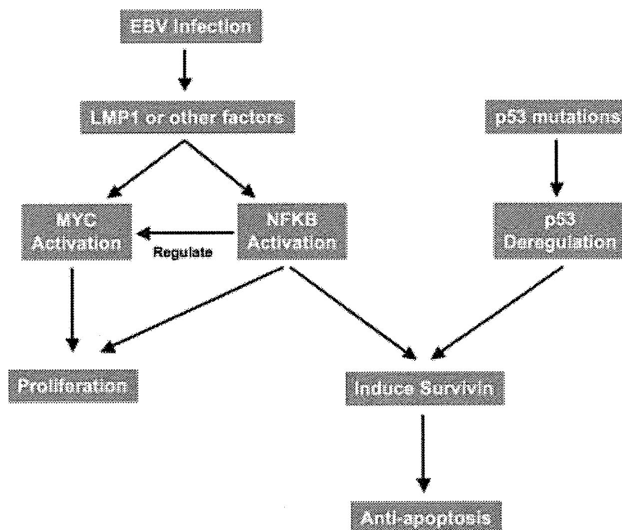

Figure 5. Model of NKTL pathogenesis involving the activation of Myc and NF-κB pathways, possibly driven by the EBV LMP-1 protein and/or other factors. In addition, the tumour acquires p53 mutations that lead to deregulated p53 function. The cumulative consequence of these oncogenic pathways results in proliferation and up-regulation of survivin, which leads to an anti-apoptotic effect on tumour cells.

Based on our findings, we propose a model of NKTL pathogenesis involving the activation of Myc and NF-κB pathways, possibly driven by the EBV LMP-1 protein (Figure 5). In addition, the tumour acquires p53 mutations that lead to deregulated p53 function. The cumulative consequence of these oncogenic pathways is the up-regulation of survivin. The impact of Myc, NF-κB, and p53 pathways on the clinical outcome of our cases is not known as our sample size was small and there was no apparent difference in survival between these groups when we correlated the data with clinical outcome (data not shown). Furthermore, as these pathways are activated in most patients, they are more likely to play a central role in pathogenesis rather than having prognostic value. Our model does not exclude the participation of other pathways in NKTL pathogenesis. Recent studies showed that activation of the STAT3 pathway is common in NKTL [11]. In our analysis, STAT3 was one of the enriched transcription factors for genes differentially expressed between NKTL and normal NK cells, although the enrichment was much weaker than Myc, p53, and NF-κB (Table 2). Of interest, survivin is also one of the downstream targets of STAT3 [45].

Positive regulatory domain I (*PRDM1*) is another gene implicated in the biology of T-cell lymphomas. Zhao *et al* recently reported that PRDM1 transcripts were detected in T- and NK-cell lymphomas and

Copyright © 2011 Pathological Society of Great Britain and Ireland. Published by John Wiley & Sons, Ltd. www.pathsoc.org.uk

PRDM1 is involved in the chemoresistance of T-cell lymphomas [46]. In corroboration with this study, our GEP data revealed an up-regulation (2.5-fold) of PRDM1 in NKTL compared with normal NK cells (see Supporting information, Supplementary Table 6). As PRDM1 is a downstream target of NF-κB and *c-MYC* is a PRDM1-targeted gene [47,48], it is interesting to postulate that the activation of NF-κB may result in the up-regulation of PRDM1 and c-MYC in NKTL. Although these pathways may not be functional in all cases of NKTL, due to tumour heterogeneity, and they may not be the only important pathways activated, they are likely to represent key events during NKTL oncogenesis. This would fit with the current clinical phenotype of NKTL, being an aggressive tumour which is largely chemoresistant and universally associated with EBV infection.

Our results also suggest that survivin may represent a useful and novel therapeutic target in NKTL. Indeed, our *in vitro* studies using a survivin inhibitor, Terameprocol, showed that successful down-regulation of survivin in KHYG-1 and NK-92 cell lines led to a significant increase in apoptosis and a decrease in viability of the tumour cells. Terameprocol is a transcription inhibitor and it selectively reduces the transcription of genes that have promoters controlled by the Sp1 factor, such as survivin [49]. It is likely that pathways other than those controlled by Sp1, such as NF-κB, p53, and STAT3, also regulate the expression of survivin in NKTL and may account for the resistance of some of the NK cell lines, such as SNK-6, to Terameprocol treatment.

In conclusion, we have identified the activation of multiple oncogenic pathways in NKTL that leads to the almost universal overexpression of survivin. The deregulation of these pathways coupled with the high levels of survivin may explain the aggressive behaviour and relative resistance of NKTL to anti-cancer therapy. In line with this hypothesis are multiple studies reporting that overexpression of survivin in tumours confers resistance to a range of anti-cancer drugs [49]. Importantly, our data suggest the possibility of using survivin as a potential therapeutic target. Multiple strategies have been employed to target the function of survivin and although clinical trials targeting survivin for cancer treatment are still in their early development, initial results are promising [49].

Acknowledgment

We express our gratitude to Ms Choo Shoa Nian from the Department of Pathology, National University of Singapore, for performing immunohistochemistry. WJC is supported by an NMRC Clinician Scientist Investigator award. SBN is supported by a National University of Singapore start-up grant (R-179-000-040-133). This work was partly supported by a Singapore Cancer Syndicate Grant (SCS-GRN102). This material is based on research/work supported by the Singapore National Research Foundation and the Ministry of Education under the Research Centre of Excellence Programme.

Author contribution statement

SBN designed the study, performed immunohistochemistry and data analysis, and wrote the paper. VS performed experiments (GEP, PCR, and cell line survivin treatment) and wrote the paper. GFH performed the gene expression analysis and wrote the paper. JBZ performed the cell line survivin treatment. ALF and ML carried out the FISH analysis. YLK, NS, and YK contributed cell lines. AK designed the study and contributed cell lines. MS-T constructed TMAs and approved the paper. WJC designed the study, performed the gene expression analysis and data analysis, and wrote the paper.

References

1. Chan JKC, Quintanilla-Martinez L, Ferry JA, *et al*. Extranodal NK/T-cell lymphoma, nasal type. In *WHO Classification of Tumours of Haematopoietic and Lymphoid Tissues* (4th edn), Swerdlow SH, Campo E, Harris NL, *et al*. (eds). IARC Press: Lyon, 2008; 285–288.
2. Kanavaros P, Briere J, Emile JF, *et al*. Epstein–Barr virus in T and natural killer (NK) cell non-Hodgkin's lymphomas. *Leukemia* 1996; **10**(Suppl 2): s84–s87.
3. Xu ZG, Iwatsuki K, Oyama N, *et al*. The latency pattern of Epstein–Barr virus infection and viral IL-10 expression in cutaneous natural killer/T-cell lymphomas. *Br J Cancer* 2001; **84**: 920–925.
4. Quintanilla-Martinez L, Kremer M, Keller G, *et al*. p53 mutations in nasal natural killer/T-cell lymphoma from Mexico: association with large cell morphology and advanced disease. *Am J Pathol* 2001; **159**: 2095–2105.
5. Takahara M, Kishibe K, Bandoh N, *et al*. P53, N- and K-Ras, and beta-catenin gene mutations and prognostic factors in nasal NK/T-cell lymphoma from Hokkaido, Japan. *Hum Pathol* 2004; **35**: 86–95.
6. Takakuwa T, Dong Z, Nakatsuka S, *et al*. Frequent mutations of *Fas* gene in nasal NK/T cell lymphoma. *Oncogene* 2002; **21**: 4702–4705.
7. Yamaguchi M, Kita K, Miwa H, *et al*. Frequent expression of P-glycoprotein/MDR1 by nasal T-cell lymphoma cells. *Cancer* 1995; **76**: 2351–2356.
8. Bossard C, Belhadj K, Reyes F, *et al*. Expression of the granzyme B inhibitor PI9 predicts outcome in nasal NK/T-cell lymphoma: results of a Western series of 48 patients treated with first-line polychemotherapy within the Groupe d'Etude des Lymphomes de l'Adulte (GELA) trials. *Blood* 2007; **109**: 2183–2189.
9. Wong KF. Genetic changes in natural killer cell neoplasms. *Leuk Res* 2002; **26**: 977–978.
10. Iqbal J, Kucuk C, Deleeuw RJ, *et al*. Genomic analyses reveal global functional alterations that promote tumor growth and novel tumor suppressor genes in natural killer-cell malignancies. *Leukemia* 2009; **23**: 1139–1151.
11. Huang Y, de Reynies A, de Leval L, *et al*. Gene expression profiling identifies emerging oncogenic pathways operating in extranodal NK/T-cell lymphoma, nasal type. *Blood* 2010; **115**: 1226–1237.

Copyright © 2011 Pathological Society of Great Britain and Ireland. Published by John Wiley & Sons, Ltd. www.pathsoc.org.uk

12. Hoshida Y, Villanueva A, Kobayashi M, *et al*. Gene expression in fixed tissues and outcome in hepatocellular carcinoma. *N Engl J Med* 2008; **359**: 1995–2004.
13. Liu X, Wang B, Ma X, *et al*. NF-kappaB activation through the alternative pathway correlates with chemoresistance and poor survival in extranodal NK/T-cell lymphoma, nasal type. *Jpn J Clin Oncol* 2009; **39**: 418–424.
14. Drexler HG, Matsuo Y. Malignant hematopoietic cell lines: *in vitro* models for the study of natural killer cell leukemia–lymphoma. *Leukemia* 2000; **14**: 777–782.
15. Matsuo Y, Drexler HG. Immunoprofiling of cell lines derived from natural killer-cell and natural killer-like T-cell leukemia–lymphoma. *Leuk Res* 2003; **27**: 935–945.
16. Fan JB, Yeakley JM, Bibikova M, *et al*. A versatile assay for high-throughput gene expression profiling on universal array matrices. *Genome Res* 2004; **14**: 878–885.
17. Bibikova M, Talantov D, Chudin E, *et al*. Quantitative gene expression profiling in formalin-fixed, paraffin-embedded tissues using universal bead arrays. *Am J Pathol* 2004; **165**: 1799–1807.
18. Tusher VG, Tibshirani R, Chu G. Significance analysis of microarrays applied to the ionizing radiation response. *Proc Natl Acad Sci U S A* 2001; **98**: 5116–5121.
19. Ekins S, Nikolsky Y, Bugrim A, *et al*. Pathway mapping tools for analysis of high content data. *Methods Mol Biol* 2007; **356**: 319–350.
20. Remstein ED, Dogan A, Einerson RR, *et al*. The incidence and anatomic site specificity of chromosomal translocations in primary extranodal marginal zone B-cell lymphoma of mucosa-associated lymphoid tissue (MALT lymphoma) in North America. *Am J Surg Pathol* 2006; **30**: 1546–1553.
21. Ambrosini G, Adida C, Sirugo G, *et al*. Induction of apoptosis and inhibition of cell proliferation by *survivin* gene targeting. *J Biol Chem* 1998; **273**: 11177–11182.
22. Chang CC, Heller JD, Kuo J, *et al*. Tetra-*O*-methyl nordihydroguaiaretic acid induces growth arrest and cellular apoptosis by inhibiting Cdc2 and survivin expression. *Proc Natl Acad Sci U S A* 2004; **101**: 13239–13244.
23. Marumoto T, Zhang D, Saya H, Aurora-A—a guardian of poles. *Nature Rev Cancer* 2005; **5**: 42–50.
24. Strebhardt K, Ullrich A. Targeting polo-like kinase 1 for cancer therapy. *Nature Rev Cancer* 2006; **6**: 321–330.
25. Malumbres M, Barbacid M, Cell cycle, CDKs and cancer: a changing paradigm. *Nature Rev Cancer* 2009; **9**: 153–166.
26. Annunziata CM, Davis RE, Demchenko Y, *et al*. Frequent engagement of the classical and alternative NF-kappaB pathways by diverse genetic abnormalities in multiple myeloma. *Cancer Cell* 2007; **12**: 115–130.
27. Huang G, Chng WJ. Predicting the oncogenic pathway activities of individual samples from microarray gene expression profiles. In *2009 International Workshop on Computational and Integrative Biology (CIB 2009)*, Hangzhou, China, 2009; 20–25.
28. Kwong YL. Natural killer-cell malignancies: diagnosis and treatment. *Leukemia* 2005; **19**: 2186–2194.
29. Li Q, Verma IM. NF-kappaB regulation in the immune system. *Nature Rev Immunol* 2002; **2**: 725–734.
30. Okamoto T, Sanda T, Asamitsu K. NF-kappa B signaling and carcinogenesis. *Curr Pharm Des* 2007; **13**: 447–462.
31. Izban KF, Ergin M, Qin JZ, *et al*. Constitutive expression of NF-kappa B is a characteristic feature of mycosis fungoides: implications for apoptosis resistance and pathogenesis. *Hum Pathol* 2000; **31**: 1482–1490.
32. Mathas S, Johrens K, Joos S, *et al*. Elevated NF-kappaB p50 complex formation and Bcl-3 expression in classical Hodgkin, anaplastic large-cell, and other peripheral T-cell lymphomas. *Blood* 2005; **106**: 4287–4293.
33. Kim K, Ryu K, Ko Y, *et al*. Effects of nuclear factor-kappaB inhibitors and its implication on natural killer T-cell lymphoma cells. *Br J Haematol* 2005; **131**: 59–66.
34. Li T, Hongyo T, Syaifudin M, *et al*. Mutations of the *p53* gene in nasal NK/T-cell lymphoma. *Lab Invest* 2000; **80**: 493–499.
35. Shen L, Au WY, Guo T, *et al*. Proteasome inhibitor bortezomib-induced apoptosis in natural killer (NK)-cell leukemia and lymphoma: an *in vitro* and *in vivo* preclinical evaluation. *Blood* 2007; **110**: 469–470.
36. Keats JJ, Fonseca R, Chesi M, *et al*. Promiscuous mutations activate the noncanonical NF-kappaB pathway in multiple myeloma. *Cancer Cell* 2007; **12**: 131–144.
37. Compagno M, Lim WK, Grunn A, *et al*. Mutations of multiple genes cause deregulation of NF-kappaB in diffuse large B-cell lymphoma. *Nature* 2009; **459**: 717–721.
38. Kaiser C, Laux G, Eick D, *et al*. The proto-oncogene c-*myc* is a direct target gene of Epstein–Barr virus nuclear antigen 2. *J Virol* 1999; **73**: 4481–4484.
39. Dirmeier U, Hoffmann R, Kilger E, *et al*. Latent membrane protein 1 of Epstein–Barr virus coordinately regulates proliferation with control of apoptosis. *Oncogene* 2005; **24**: 1711–1717.
40. Devergne O, Hatzivassiliou E, Izumi KM, *et al*. Association of TRAF1, TRAF2, and TRAF3 with an Epstein–Barr virus LMP1 domain important for B-lymphocyte transformation: role in NF-kappaB activation. *Mol Cell Biol* 1996; **16**: 7098–7108.
41. Faumont N, Durand-Panteix S, Schlee M, *et al*. c-Myc and Rel/NF-kappaB are the two master transcriptional systems activated in the latency III program of Epstein–Barr virus-immortalized B cells. *J Virol* 2009; **83**: 5014–5027.
42. Andersen MH, Svane IM, Becker JC, *et al*. The universal character of the tumor-associated antigen survivin. *Clin Cancer Res* 2007; **13**: 5991–5994.
43. Paydas S, Ergin M, Erdogan S, *et al*. Thrombospondin-1 (TSP-1) and survivin (S) expression in non-Hogkin's lymphomas. *Leuk Res* 2008; **32**: 243–250.
44. Raj D, Liu T, Samadashwily G, *et al*. Survivin repression by p53, Rb and E2F2 in normal human melanocytes. *Carcinogenesis* 2008; **29**: 194–201.
45. Zhou J, Bi C, Janakakumara JV, *et al*. Enhanced activation of STAT pathways and overexpression of survivin confer resistance to FLT3 inhibitors and could be therapeutic targets in AML. *Blood* 2009; **113**: 4052–4062.
46. Zhao WL, Liu YY, Zhang QL, *et al*. PRDM1 is involved in chemoresistance of T-cell lymphoma and down-regulated by the proteasome inhibitor. *Blood* 2008; **111**: 3867–3871.
47. Johnson K, Shapiro-Shelef M, Tunyaplin C, *et al*. Regulatory events in early and late B-cell differentiation. *Mol Immunol* 2005; **42**: 749–761.
48. Lin Y, Wong K, Calame K. Repression of c-myc transcription by Blimp-1, an inducer of terminal B cell differentiation. *Science* 1997; **276**: 596–599.
49. Ryan BM, O'Donovan N, Duffy MJ. Survivin: a new target for anti-cancer therapy. *Cancer Treat Rev* 2009; **35**: 553–562.

Copyright © 2011 Pathological Society of Great Britain and Ireland.
Published by John Wiley & Sons, Ltd. www.pathsoc.org.uk

SUPPORTING INFORMATION ON THE INTERNET

The following supporting information may be found in the online version of this article.

Supplementary methods.

Table S1. Clinical data of nasal-type extranodal natural killer/T-cell lymphoma study cases.

Table S2. Immunohistochemistry: antibodies and staining conditions.

Table S3. Characteristics of cell lines derived from NK-cell neoplasm used in this study.

Table S4. Primers used for PCR validation.

Table S5. BAC clones used to prepare fluorescence *in situ* hybridization probes.

Table S6. Genes differentially expressed between NKTCL and normal NK cells.

Table S7. Summary of results for immunohistochemistry for c-Myc, p53, NF-κB proteins, and survivin in NKTL samples.

Table S8. Summary of results for immunohistochemistry for c-Myc, p53, NF-KB proteins, and survivin in normal NK cells.

Figure S1. Quantitative PCR validation of several candidate genes showed that on the whole this is consistent with gene expression data showing higher expression of EZH2, STMN1, and BIRC5 (survivin) in NKTL compared with unstimulated and stimulated normal NK cells.

Figure S2. A heat map of normalized iPASA scores.

Figure S3. Expression of leading contributing genes from the enriched metastasis related gene sets.

Figure S4. Comparison of gene expression-based MYC index with MYC staining by immunohistochemistry.

Copyright © 2011 Pathological Society of Great Britain and Ireland.
Published by John Wiley & Sons, Ltd. www.pathsoc.org.uk

Lab on a Chip

View Online
Dynamic Article Links

Cite this: DOI: 10.1039/c0lc00519c

www.rsc.org/loc

TECHNICAL NOTE

Point-of-care testing system enabling 30 min detection of influenza genes†

Tomoteru Abe,[a] Yuji Segawa,[a] Hidetoshi Watanabe,[a] Tasuku Yotoriyama,[a] Shinichi Kai,[b] Akio Yasuda,[a] Norio Shimizu[c] and Naoko Tojo[d]

Received 19th October 2010, Accepted 7th January 2011
DOI: 10.1039/c0lc00519c

Published on 11 February 2011 on http://pubs.rsc.org | doi:10.1039/C0LC00519C
Downloaded on 14 February 2011

We developed a portable and easy-to-use nucleic acid amplification test (NAT) system for use in point-of-care testing (POCT). The system shows sensitivity that is sufficiently higher than that of the currently available rapid diagnostic kit and is comparable to that of real-time reverse transcription polymerase chain reaction (RT-PCR) for influenza testing.

Currently, a rapid diagnostic kit employing immuno-chromatography is used in the diagnosis of infectious diseases (*e.g.*, influenza) and is widely used as a point-of-care test (POCT) because of its convenience and rapidity. However, this testing method has low sensitivity (*e.g.*, 40–69% for detection of influenza A)[1] and does not provide genetic information (*e.g.*, virus subtype, drug resistance) about the clinical sample. Furthermore, although reverse transcription polymerase chain reaction (RT-PCR) is used as a nucleic acid amplification test (NAT),[2] it is only applied to clinically important specimens due to the complexity of the procedures and time requirements. Our rapid testing system is portable, easy-to-use, and will allow quicker and more appropriate treatment.

Our NAT system comprises a disposable chip with multiple reaction wells, a heater, an optical system to measure fluorescence and a control system (Fig. 1a). An indium tin oxide (ITO) thin film on glass is used as the heater and to accommodate a transparent optical system. The optical components, including LEDs for excitation of fluorescent dye, photo-diodes for detection of fluorescent signal and lenses for focusing and collimating, are positioned to correspond to each well, which contributes to the miniaturization of the system (Fig. 1b). The disposable chip has a glass–polydimethylsiloxane (PDMS)–glass microfluidic structure and nine interconnected 1 μL reaction wells (Fig. 2a). The PDMS structure is bonded to the upper and lower glass in a vacuum chamber at less than 0.01 atm to produce an internal pressure of both the channel and wells of approximately 0.01 atm, which eliminates the need for pumps and tubing for injection of sample solution (Fig. 2b). Using vacuum aspiration, a nasopharyngeal swab sample extracted in solution including SYBR Green I is injected by a disposable injector with a needle to an injection port in the PDMS layer and can be loaded to all reaction wells within 10 s. Sample contamination among chips is

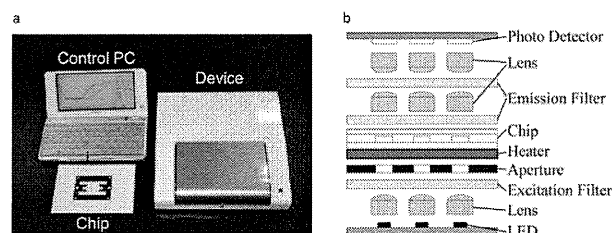

Fig. 1 POC NAT system and optical system. (a) The system includes a device for heating samples and detecting fluorescence, a laptop for controlling the system and disposable testing chips. (b) Cross-sectional view of the reaction and detection unit. Each well is equipped with a dedicated optical system: light from the LEDs is passed through a collimating lens directed to the sample, and excitation fluorescence is detected with photo-diodes.

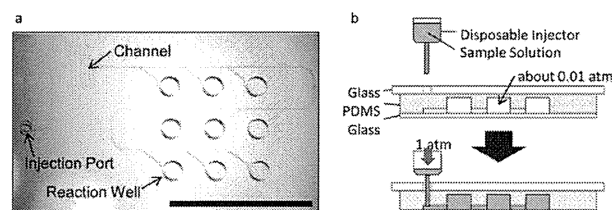

Fig. 2 The disposable testing chip. (a) The channel and reaction wells on the chip (scale bar = 1 cm). (b) Cross-sectional view of the disposable testing chip and conceptual diagram of sample injection. The interior pressure of both the channel and wells is maintained at approximately 0.01 atm. A sample solution can easily be loaded to the inlet of the chip and loads to all reaction wells within 10 s due to the vacuum aspiration. The self-sealing PDMS layer prevents fluid from escaping once the needle is removed.

[a]*Sony Corporation, Life Science Laboratory, Advanced Materials Laboratories, Tokyo Medical and Dental University, 1-5-45 Yushima, Bunkyo-ku, Tokyo, 113-8510, Japan*
[b]*Sony Corporation, Core Device Development Group, Life Electronics Business Development Department, 5-1-12 Kita-shinagawa, Shinagawa-ku, Tokyo, 141-0001, Japan*
[c]*Tokyo Medical and Dental University, Medical Research Institute, 1-5-45 Yushima, Bunkyo-ku, Tokyo, 113-8510, Japan*
[d]*Tokyo Medical and Dental University Hospital of Medicine, Department of Clinical Laboratory, 1-5-45 Yushima, Bunkyo-ku, Tokyo, 113-8510, Japan*

† Electronic supplementary information (ESI) available. See DOI: 10.1039/c0lc00519c

extremely unlikely because there is no outlet port. Loop-mediated isothermal amplification (LAMP), which has been reported to be a rapid, accurate and cost-effective method for diagnosing infectious diseases,[3,4] was adopted for nucleic acid amplification. The RNA amplification reagent (desiccant type) developed based on the LAMP method and primer sets for the influenza virus that have been commercialized for laboratory use were incorporated into our POC NAT system. The chip was prepared by aliquoting suitable quantities of primer mix (PM) and enzyme mix (EM) solutions (gifts from Eiken Chemical, Japan) for a 1 μL reaction to each well of the chip and desiccating these solutions. Thus, the chip has solid state reagents, avoiding the need for pipette work during analysis. As no purification of the clinical sample is necessary in this procedure, results can be obtained in 30 min.

In order to validate the practicability of our POC NAT system, we conducted two series of tests using clinical specimens. Seventy-seven patients (33 males and 44 females; mean age 33.4 years, range 3–89 years) with respiratory symptoms who visited the Tokyo Medical and Dental University Hospital outpatient clinic between December 2009 and February 2010 provided samples for these study. (Informed consent was obtained from these patients prior to sample collection.) First, we attempted to detect multiple genes on one chip (Fig. 3). We then used the residual solution of 45 nasopharyngeal swab samples from a rapid diagnostic test kit (ESP-LINE Influenza A&B-N rapid diagnostic test kit: Fujirebio, Japan) to compare the POC NAT system and real-time RT-PCR detection. RNA from 140 μL of residual solution from the kit was purified by QIAamp Virus RNA Mini kit (QIAGEN, USA), and 3 μL of the purified RNA solution with Loopamp Extraction Reagent for Influenza Virus (EX) (Eiken Chemical, Japan) containing SYBR

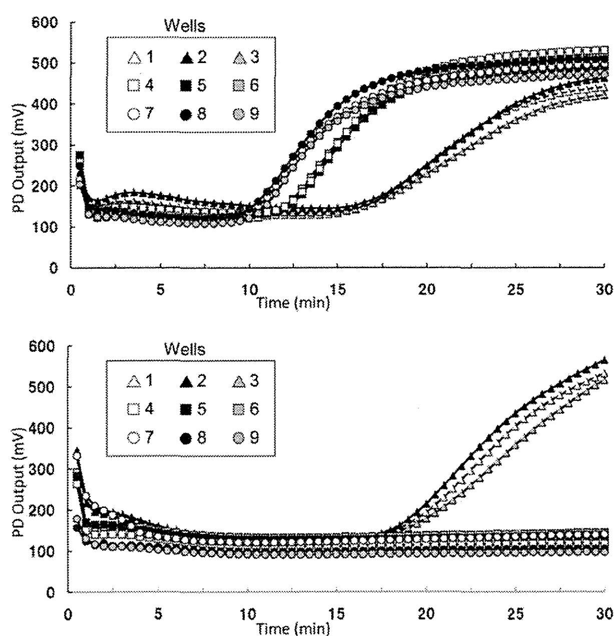

Fig. 3 Typical results from influenza testing for a positive result (upper panel) and a negative result (lower panel). The increase of output voltage indicates increased fluorescence corresponding to nucleic acid amplification. In the example shown, wells 1–3 were spotted with human β-actin primer, wells 4–6 were spotted primers specific to pandemic influenza and wells 7–9 were spotted consensus primers to influenza A.

Green I was used to the POC NAT system containing EM with PM for human β-actin (ACTB) in wells 1–3, PM for H1pdm 2009 influenza (H1) in wells 4–6, and PM for influenza A (FluA) in wells 7–9. RT-PCR was conducted according to the WHO-recommended protocol[5] using 5 μL of the purified RNA solution. RT-PCR and the POC NAT system produced the same diagnostic results for 42 of 45 specimens. There were no false-positive results, indicating that there was no cross-contamination among the reaction wells (Table 1, ESI†). Next, we compared the sensitivities of RT-PCR and our NAT system and rapid diagnostic test kit. First, we suspended 42 nasopharyngeal swab samples in 130 μL of virus transfer medium (VTM: MEM medium base, including 0.5% BSA, 500 U mL^{-1} penicillin, 500 μg mL^{-1} streptomycin, 100 mg mL^{-1} gentamicin, and 2 μg mL^{-1} amphotericin B) and then suspended 40 μL of the VTM/sample suspension mixture in 4 mL of EX with SYBR Green I; 6 μL of this mixture was used to test the POC NAT system. Each well of the testing chips contained solid phase reagent: specifically, EM in all 9 wells, PM for H1 in wells 1–8, and ACTB in well 9. In parallel, 40 μL of the VTM/sample suspension mixture was resuspended in 2 mL of fresh VTM, and 140 μL of this solution was subjected to RT-PCR by the WHO-recommended protocol.[5] The POC NAT system successfully detected 20 out of 22 influenza-positive specimens, as determined by RT-PCR. Based on a total of 42 specimens tested (Table 1, ESI†), the sensitivity of our system is approximately 90.9% (20 of 22 RT-PCR positive samples). On the other hand, the sensitivity of rapid diagnostic test kit is estimated from the test results of the other swab samples from seventy-seven patients. In this study, we used the residual solution of 77 nasopharyngeal swab samples from a rapid diagnostic test kit (ESP-LINE Influenza A&B-N rapid diagnostic test kit: Fujirebio, Japan) to compare the real-time RT-PCR detection. RNA from 140 μL of residual solution from the kit was purified by QIAamp Virus RNA Mini kit, and RT-PCR was conducted according to the WHO-recommended protocol[5] using 5 μL of the purified RNA solution. The sensitivity of the kit in our study is approximately 78.6% (33 of 42 RT-PCR positive samples).

We presented herein a POC NAT system that offers a solution to the problems associated with the commonly used rapid diagnosis kit and conventional NATs. Our POC NAT system is as easy to operate as the rapid diagnostic kit, and testing with the new system is completed in 30 min. Moreover, information regarding multiple genes can be obtained from a single test. Finally, the detection sensitivity of our POC NAT system is significantly higher than that of the rapid diagnostic kit and is comparable to that of RT-PCR. The technology utilized in the development of our NAT system will not only benefit current medical diagnostic procedures but will also be applicable to the detection of infectious diseases, such as tuberculosis and HIV, in developing countries that lack effective diagnostic procedures.

References

1 Centers for Disease Control and Prevention (CDC), *MMWR Morb. Mortal. Wkly. Rep.*, 2009, **58**, 826.
2 J. Versalovic and J. R. Lupski, *Trends Microbiol.*, 2002, **10**, S15.
3 T. Notomi, H. Okayama, H. Masubuchi, T. Yonekawa, K. Watanabe, N. Amino and T. Hase, *Nucleic Acids Res.*, 2000, **28**, E63.
4 Y. Mori and T. Notomi, *J. Infect. Chemother.*, 2009, **15**, 62.
5 World Health Organization, *WHO Information for Laboratory Diagnosis of Pandemic (H1N1) 2009 Virus in Humans—Revised*, World Health Organization, 23 November 2009.

Published on 11 February 2011 on http://pubs.rsc.org | doi:10.1039/C0LC00519C

This journal is © The Royal Society of Chemistry 2011

Ann Hematol (2011) 90:851–852
DOI 10.1007/s00277-010-1095-x

LETTER TO THE EDITOR

Autoimmune hemolytic anemia and autoimmune neutropenia in a child with erythroblastopenia of childhood (TEC) caused by human herpesvirus-6 (HHV-6)

Hiroshi Yagasaki · Maiko Kato · Norio Shimizu · Hiroyuki Shichino · Motoaki Chin · Hideo Mugishima

Received: 20 September 2010 / Accepted: 23 September 2010 / Published online: 5 October 2010
© Springer-Verlag 2010

Dear Editor,
Transient erythroblastopenia of childhood (TEC) is a self-limiting disorder of young children that is characterized by moderate to severe anemia with reticulocytopenia and decreased numbers of erythroid precursors in the bone marrow. TEC was often complicated with neutropenia and thrombocytopenia [1–3]. Here, we document a unique clinical course in a child with TEC.

A 1-year-old girl with anemia was admitted to our hospital. She had no recent episodes of viral infection such as fever and skin eruption. The values for hemoglobin (Hb) and reticulocytes were 57 g/L and 2.0% (Table 1). Although the direct Coombs test was highly positive, the haptoglobin level remained normal. In addition, the leukocyte fraction indicated agranulocytosis. Bone marrow findings were as follows: cellularity was normocellular, the erythroid series were reduced (M/E ratio, 4.2), and the myeloid series differentiated to a band form but not segmental neutrophils.

Speculating that viral infection was involved in this bicytopenia, we performed multiplex PCR analyses for the following viruses: herpes simplex virus type 1, type 2, human herpesvirus type 6 (HHV-6), type 7, type 8, varicella-zoster virus, Epstein-Barr virus (EBV), cytomegalovirus, parvovirus B19, polyomavirus JC, and polyomavirus BK, as described previously [4]. As a result, HHV-6 DNA (10×10^4 copies/μg DNA) was detected in the peripheral whole blood. Because we assumed that HHV-6 infection suppressed erythropoiesis, we started ganciclovir (GCV) from day 15. The reticulocyte count responded rapidly to GCV and increased to 10.8% on day 22 (Table 1). The HHV-6 DNA level also decreased significantly (0.84×10^4 copies/μg DNA); however, the Hb level decreased to 40 g/L on day 25.

As the haptoglobin level decreased, a diagnosis of hemolytic crisis was made. High-dose globulin (total dose, 1.5 g/kg) was given on days 25 to 27 with subsequent standard steroid therapy on days 37 to 74. The hemolysis resolved rapidly, and the Hb level increased up to 89 g/L on day 33. Coombs test became negative by day 67, and the patient was discharged on day 74. The level of HHV-6 antibody increased during this episode, which indicated a primary infection of HHV-6 (Table 1).

At present (day 273), the patient has no relapse of anemia. In contrast, the neutrophil count did not change. Anti-neutrophil antibodies were identified by flow cytometric analysis, which was consistent with autoimmune neutropenia.

The association between TEC and viral infection such as parvovirus B19, EBV, cytomegalovirus, and HHV-6 has been raised in few patients [5–7]. In our patient, HHV-6 infection was proven by a molecular technique and successfully treated using GCV. Another notable feature is that this patient presented with autoimmune hemolytic anemia and neutropenia, concurrently. We speculated that the immune response against HHV-6 has stimulated the production of multiple autoantibodies against red cells and

H. Yagasaki (✉) · M. Kato · H. Shichino · M. Chin · H. Mugishima
Department of Pediatrics, Nihon University,
Ohtaniguchi 30-1,
Itabashi-ku, Tokyo, Japan 173-8610
e-mail: yagasaki@med.nihon-u.ac.jp

N. Shimizu
Department of Virology, Medical Research Institute,
Tokyo Medical and Dental University,
Tokyo, Japan

Table 1 Laboratory results

	Normal range	Day 1[a]	Day 15	Day 22	Day 25	Day 33	Day 46	Day 67	Day 273
Hb (g/L)		57	52	47	40	89	91	108	122
Reticulocyte (%)		2	2.8	10.8	7.2	9	4.2	1.4	1.3
White blood cell (× 109/L)		4.6	7.5	3.1	4.4	4.7	6.2	5.8	5.3
Neutrophil (%)		0	0	0	0	2	0	0	2
Eosinophil (%)		1.5	0	1	2	0	0	4	1
Basophil (%)		0.5	0	0	0	0	0	1	0
Monocyte (%)		9	22	9	3	5	5	27	20
Lymphocyte (%)		85	77.5	90	95	93	94	68	77
Atypical lymphocyte (%)		4							
Platelet (× 109/L)		266	543	320	238	378	513	322	226
Total bilirubin (mg/dL)	0.3–1.2	0.5	0.62	1.32	0.65	0.93	0.36	0.35	0.21
Lactate dehydrogenase (U/L)	106–220	419	226	320	297	351	226	227	269
Coombs test (direct)		4+	4+	4+		3+	2+	–	–
Haptoglobin (mg/dL)	25–176	201	146		80	10	83	157	84
Erythropoietin (mU/mL)	8–36	1,460					86		
HHV-6 antibody (IgG)						<10	80	160	640

[a] Day 1 is the day of admission

neutrophils. Interestingly, marked hemolysis occurred just after the erythroid suppression was resolved. Because the structure and properties of the plasma membrane change extensively in the transition of reticulocytes into mature erythrocytes, the active target of hemolysis in this patient may be a molecule on reticulocytes rather than on mature red cells [8].

Conflicts of interest All authors have neither conflicts of interest nor financial support.

References

1. Hanada T, Koike K, Hirano C et al (1989) Childhood transient erythroblastopenia complicated by thrombocytopenia and neutropenia. Eur J Haematol 42:77–80
2. Rogers ZR, Bergstrom SK, Amylon M et al (1989) Reduced neutrophil counts in children with transient erythroblastopenia of childhood. J Pediatr 115:746–748
3. Cherrick I, Karayalcin G, Lanzkowsky P (1994) Transient erythroblastopenia of childhood. Prospective study of fifty patients. Am J Pediatr Hematol Oncol 16:320–324
4. Sugita S, Shimizu N, Watanabe K et al (2008) Use of multiplex PCR and real-time PCR to detect human herpes virus genome in ocular fluids of patients with uveitis. Br J Ophthalmol 92:928–932
5. Prassouli A, Papadakis V, Tsakris A et al (2005) Classic transient erythroblastopenia of childhood with human parvovirus B19 genome detection in the blood and bone marrow. J Pediatr Hematol Oncol 27:333–336
6. Penchansky L, Jordan JA (1997) Transient erythroblastopenia of childhood associated with human herpesvirus type 6, variant B. Am J Clin Pathol 108:127–132
7. Skeppner G, Kreuger A, Elinder G (2002) Transient erythroblastopenia of childhood: prospective study of 10 patients with special reference to viral infections. J Pediatr Hematol Oncol 24:294–298
8. Liu J, Guo X, Mohandas N et al (2010) Membrane remodeling during reticulocyte maturation. Blood 115:2021–2027

Leukemia (2011) 25, 1324–1334
© 2011 Macmillan Publishers Limited All rights reserved 0887-6924/11
www.nature.com/leu

ORIGINAL ARTICLE

The role of microRNA-150 as a tumor suppressor in malignant lymphoma

A Watanabe[1,6], H Tagawa[1,6], J Yamashita[2], K Teshima[1], M Nara[1], K Iwamoto[1], M Kume[3], Y Kameoka[1], N Takahashi[1], T Nakagawa[4], N Shimizu[5] and K Sawada[1]

[1]Department of Hematology, Nephrology and Rheumatology, Akita University Graduate School of Medicine, Akita, Japan; [2]Radioisotope Research Laboratory, Bioscience Education-Reserch Center, Akita University, Akita, Japan; [3]Department of Internal Medicine, Hiraka General Hospital, Akita, Japan; [4]Department of Surgery, Senboku Kumiai General Hospital, Akita, Japan and [5]Division of Virology and Immunology, Medical Research Institute, Tokyo Medical and Dental University, Tokyo, Japan

MicroRNA (miRNA; miR) is a class of small regulatory RNA molecules, the aberrant expression of which can lead to the development of cancer. We recently reported that overexpression of miR-21 and/or miR-155 leads to activation of the phosphoinositide 3-kinase (PI3K)–AKT pathway in malignant lymphomas expressing $CD3^-CD56^+$ natural killer (NK) cell antigen. Through expression analysis, we show in this study that in both NK/T-cell lymphoma lines and samples of primary lymphoma, levels of miR-150 expression are significantly lower than in normal NK cells. To examine its role in lymphomagenesis, we transduced miR-150 into NK/T-cell lymphoma cells, which increased the incidence of apoptosis and reduced cell proliferation. Moreover, the miR-150 transductants appeared senescent and showed lower telomerase activity, resulting in shortened telomeric DNA. We also found that miR-150 directly downregulated expression of *DKC1* and *AKT2*, reduced levels of phosphorylated $AKT^{ser473/4}$ and increased levels of tumor suppressors such as Bim and p53. Collectively, these results suggest that miR-150 functions as a tumor suppressor, and that its aberrant downregulation induces continuous activation of the PI3K–AKT pathway, leading to telomerase activation and immortalization of cancer cells. These findings provide new insight into the pathogenesis of malignant lymphoma.
Leukemia (2011) **25,** 1324–1334; doi:10.1038/leu.2011.81; published online 19 April 2011
Keywords: miR-150; microRNA; malignant lymphoma; NK/T-cell lymphoma; AKT2; senescence

Introduction

The genes responsible for T-cell and natural killer (NK)-cell lymphoma/leukemia are largely unknown because specific translocations have not yet been identified, although analyses to determine genomic copy number alterations revealed a 6q21 deletion, which is seen in about 10–20% of T and NK/T-cell lymphomas.[1–8]

Cancer cells gain a survival advantage by adding to abilities such as cell proliferation, anti-apoptotic function and immortalization. These changes are caused by altering the expression of oncogenes and/or tumor suppressor genes/proteins, such as c-Myc, Bcl2 and p53, among many others. In addition, recently discovered microRNAs (miRNAs) are known to associate with tumorigenesis and to alter the expression of both oncogenes and tumor suppressor genes.[9–12]

Correspondence: Dr H Tagawa, Department of Hematology, Nephrology and Rheumatology, Akita University Graduate School of Medicine, Akita 0108543, Japan.
E-mail: htagawa0279jp@yahoo.co.jp
[6]These authors contributed equally to this work.
Received 30 November 2010; revised 16 February 2011; accepted 15 March 2011; published online 19 April 2011

miRNAs are a class of small RNA molecules that have a regulatory function and have important roles in tumor development by pairing with the 3′-untranslated region (UTR) of target mRNAs to repress their productive translation.[9–12] Various miRNA alterations have been identified in lymphoma/leukemias, as well as in solid tumors, irrespective of the presence or absence of disease-specific genomic/genetic alterations.[9–12] We recently observed that two oncomiRs (miR-21 and miR-155) are overexpressed in NK/T-cell lymphoma, and that they contribute to lymphomagenesis by enhancing anti-apoptotic function. These miRNAs downregulate phosphatase and tensin homolog (PTEN), programmed cell death 4 and Src homology-2 domain-containing inositol 5-phosphatase 1 (SHIP1) while upregulating phosphorylated $AKT^{ser473/4}$.[13] These findings suggest that activation of the phosphoinositide 3-kinase (PI3K)–AKT pathway is important for NK/T-cell lymphomagenesis. Consistent with that idea, Huang *et al.*[14] recently used gene expression profiling to show the importance of activation of PI3K–AKT pathway in NK/T-cell lymphoma. Taken together, these results suggested miR-21 and miR-155 are upstream regulators of PI3K–AKT signaling.

In that context, the aim of the present study was to investigate the role of aberrantly downregulated miRNAs in T- and NK-cell lymphoma by using miRNA arrays, Northern blotting and quantitative PCR to examine miRNA expression in NK-cell and $CD56^+$ T-cell lymphoma lines. We found that expression of miR-150 is significantly diminished in both cell lines and in samples of primary lymphoma. We then tested the effects of transducing miR-150 to NK/T-cell lymphoma lines to determine whether it might function as a tumor suppressor.

Materials and methods

Lymphoma cell lines

NK and NK/T-cell lymphoma lines. We used 11 cell lines as NK/T-cell lymphoma leukemia cell lines, which are commonly showing $CD2^+$, $sCD3^-$, $CD3\varepsilon^+$, $CD5^-$, $CD56^+$, $TCR\alpha\beta^-$ and $TCR\gamma\delta^-$ phenotypes, including NKL, KHYG-1, YT, KAI-3, NK-92, HANK-1, SNK-1, SNK-6, DERL-7, SNK-10 and MOTN-1.[13–18] Of these, YT, KAI-3, HANK-1, SNK-1, SNK-6 and SNK-10 are EBV^+.[15,16] Although MOTN-1 was established from T-cell large granular lymphocyte leukemia, the cell line is showing NK-cell antigen.[17]

$CD56^+$ T-cell lymphoma lines. We also used five $CD56^+$ T-cell lymphoma lines including MTA, SNT-8, SNT-13, SNT-15 and SNT-16 cells, which are $sCD3^+CD56^+$ T-cell lymphoma cells showing T-cell receptor rearrangement.[18] MTA and

SNT-16 are TCR$\alpha\beta^+$, whereas the remaining cells are TCR$\gamma\delta^+$.[13] SNT-8, SNT-13, SNT-15 and SNT-16 cells are EBV$^+$.[18]

B-cell lymphoma cell lines. Raji and Daudi were derived from sporadic Burkitt lymphoma (EBV$^+$). Information of lymphoma cell lines used for this experiment is described in Supplementary Table 1.

Primary lymphoma samples and normal NK and T cells NK/T-cell lymphoma/leukemia. Nine samples of 'extranodal NK/T cell lymphoma, nasal type' and three samples of 'aggressive NK-cell leukemia' were collected from 12 patients. Out of 12 cases, 11 were previously used for miRNA analysis.[13] The remaining one case is described in Results section in this paper. These samples were positive for CD56, EBV infection or cytotoxic molecules such as TIA1 and GranzymeB. T cells showing the sCD3 ($n=15$) and NK cells showing the sCD3$^-$CD56$^+$ phenotype ($n=14$) were also collected from healthy donors using a magnetic cell sorting system (Miltenyi Biotec., Bergisch Gladbach, Germany)or cell sorter (Dako Cytomation MoFlo; Dako, Glostrup, Denmark). Polyclonal IL-2-activated NK cells were expanded in Iscove's modified Dulbecco's medium (Invitrogen, Carlsbad, CA, USA) supplemented with 10% human serum, 100 U/ml recombinant IL-2 (Hoffmann-La Roche, Basel, Switzerland) and 10% purified human IL-2 (Hemagen, Columbia, MD, USA). Resting NK cells were resuspended in the same medium without IL-2 and were used within 4 days after isolation. These cells were 95–99% CD3$^-$CD56$^+$, as determined by flow cytometry. All the samples were obtained from tumors at the time of diagnosis before any treatment was administered. Samples were obtained under protocol approved by the Institutional Review Board of Akita University.

miRNAs expression analyses

We performed miRNA array, Northern blot analysis and Taqman PCR analysis. Detail is described in Supplementary Methods. Ninety probes used for Northern blot and expression pattern of miRNAs are described in Supplementary Table 2.

Construction of plasmids and transduction

Lentiviral vectors for the delivery of miRNAs were designed and produced using the reagents and protocols included in the BLOCK-iT Lentiviral Pol II miR RNA interference expression system (Invitrogen). Detailed method is described in Supplementary Methods. The premicro-RNA (miR-150) inserted vector was transfected using Lipofectamine 2000 into 293FT producer cells. After overnight culture, the medium was replaced to remove the transfection reagents, and viral supernatants were collected the following day (72 h after transfection). Viral supernatants were applied to lymphoma cell lines. After removing the medium, the cells were cultured for an additional 48 h, and green fluorescent protein (GFP)$^+$ cells were collected using a cell sorter (Dako Cytomation MoFlo). In this study, we defined 'day 0' as the day on which lymphoma cells were sorted for GFP-miR-150 positivity: 48 h after either miR-150-GFP or GFP infection.

Antisense oligonucleotide assays

Antisense oligonucleotides (ASOs) and their respective scrambled control oligonucleotides were synthesized as hybrid deoxyribonucleotide molecules linked between the 2′-O and 4′-C-methylene bridge (locked nucleic acid) modification of G and C residues (Greiner, Tokyo, Japan) as described previously.[13,19]

Cell growth assay

Transduced cells (1.0×10^3/well, MOTN-1, SNK-6 and HANK-1) cultured in 96-well plates were transferred to 12-well plates, after which viable cells were identified by trypan blue exclusion and counted on days from 0 to 63 from miR-150 selection (at 2–65 days after transduction).

Cell proliferation assay (5′-bromo-2′-deoxyuridine assay)

Cell proliferation was assessed using a BrdU Cell Proliferation Assay kit (Merck, Darmstadt, Germany) following the manufacturer's protocol.

Apoptosis assay

An annexin V-PE apoptosis detection kit (BD Biosciences, San Jose, CA, USA) was used to assess the incidence of apoptosis among GFP$^+$ cells. Cells were exposed to 100 μM etoposide for 4 h, after which the assays were carried out.

Senescence-associated β-gal assay

Senescence-associated beta-gal was assayed using a Senescence Detection Kit (BioVision, Mountain View, CA, USA) according to the manufacturer's protocol.

Telomerase activity (telomeric repeat amplification protocol) assay

Telomerase activity was assayed using a TRAP$_{EZE}$ Gel-Based Telomerase Detection Kit (Millipore, Billerica, MA, USA). Cells (3×10^5) were suspended in CHAPS lysis buffer, and PCR was performed according the manufacturer's instructions.

Southern blot analysis

DNA (5 μg) was digested with *Hin*fI and transferred to Hybond N membranes (GE Healthcare Japan, Tokyo, Japan).

Western blot analysis

Antibodies against phospho-AKT$^{ser473/4}$ (pAKT), total AKT, AKT2 and c-Myc were all purchased from Cell Signaling Technology (Danvers, MA, USA; Cell Cycle Regulation Sampler Kit). Anti-p53 (DO-7) was from Dako Cytomation and anti-Bim (AAP-330) was from Stressgen Bioreagents (Funakoshi, Tokyo, Japan). Dyskerin (gene name: *DKC1*) was purchased from Santa Cruz Biotechnology (Santa Cruz, CA, USA).

Luciferase reporter assay

Double-stranded oligonucleotides corresponding to the wild-type (WT-3′-UTR) or mutant (MUT-3′-UTR) miR-150 binding site in the *DKC*1 of 3′-UTRs were synthesized (Sigma-Aldrich, St Louis, MO, USA) and ligated between the *Spe*I and *Hin*dIII restriction sites of the reporter plasmid pMIR-REPORT (Ambion, St Austin, TX, USA). 3′-UTR of mutated and wild-type AKT2 was amplified by PCR. Sequences of 3′-UTRs of the target genes of *DKC1* and *AKT2* are shown in Supplementary Table 3.

Results

Detection of candidate tumor suppressor miRNAs in NK/T-cell lymphomas

To identify aberrant expression of miRNAs in NK/T-cell lymphomas/leukemias, we initially carried out miRNA arrays with normal (sCD3$^-$CD56$^+$) NK cells and seven NK/T-cell lymphoma/leukemia lines (YT, KAI-3, KHYG-1, NKL, NK-92, HANK-1 and SNK-6). We found that expression of 37 out of 858 hsa-miRNAs was recurrently (two and more) reduced in the lymphoma cells, as compared with normal NK cells (Supplementary Table 2). To validate the expression of these miRNAs in NK/T-cell lymphomas/leukemias, we carried out Northern analyses with normal NK, T-cell and various lymphoma lines using 90 probe sets, which included candidate oncomiRs in various cancers (let-7, miR-15, miR-221 and so on),[10–12] as well as hematopoietic-specific miRNAs (miR-16, miR-451 and miR-223 and so on) (Supplementary Table 2).[20,21] The lymphoma cell lines used included those showing a sCD3$^-$CD56$^+$ phenotype (YT, KAI-3, NK-92, NKL, DERL-7, HANK-1, MOTN-1 and SNK-6), two T-cell lymphoma/leukemia lines (sCD3$^+$) (MyLa and JM) and two B-cell lymphoma lines (Raji and Daudi). Figure 1 shows the miRNA expression in four samples of normal/resting NK (sCD3$^-$CD56$^+$) cells and eight sCD3$^-$CD56$^+$ lymphoma lines. Northern analyses revealed that let-7e, miR-29c, miR-30e, miR-125a, miR-150, miR-181a and miR-223 were more highly expressed in NK cells than in the sCD3$^-$CD56$^+$ lymphoma cell lines. These differences were particularly evident in the case of miR-150 in NK-cell. For these candidate miRNAs, we also conducted Taqman quantitative PCR analysis using RNA collected from normal NK cells ($n=11$), NK/T-cell lymphoma/leukemia lines ($n=11$), and primary NK/T-cell lymphoma samples ($n=11$) (Supplementary Figure 1). This analysis confirmed that expression of miR-150, but not the other miRNAs tested, was significantly ($P<0.05$) higher in normal NK cells than in either the lymphoma cell lines or the primary lymphoma samples.

Aberrantly reduced expression of miR-150 in NK/T-cell lymphoma

Quantitative PCR revealed high levels of miR-150 expression in normal sCD3$^+$T, and sCD3$^-$CD56$^+$ NK cells. Figure 2a summarizes a set of quantitative PCR analyses carried out with NK cells (sCD3$^-$CD56$^+$) ($n=14$), T cells (sCD3$^+$) ($n=15$), NK/T-cell lymphoma lines (sCD3$^-$CD56$^+$TCR$^-$) ($n=11$) and CD56$^+$ T-cell lymphoma (sCD3$^+$CD56$^+$TCR$^+$) lines ($n=5$), as well as samples of primary NK/T-cell lymphoma/leukemia ($n=12$). We also compared expression of miR-150 in resting and activating NK cells and found that both the groups showed strong expression of miR-150, and that there was no significant difference between them (Figure 2b). The results show that the level of miR-150 expression in normal T and NK cells was significantly ($P<0.05$) higher than in the cell lines and primary lymphoma samples. For example, Northern analysis confirmed the reduced expression of miR-150 in a primary case of NK/T-cell lymphoma extranodal type (56-year-old female), showing positivity for pAKT, CD56, TIA-1 and EBV (Supplementary Figure 2). After collecting NK cells from the patient's peripheral blood, and taking tumor specimens from her nasal cavity, Northern analysis showed miR-150 expression to be markedly low than in normal NK cells. Notably, this patient showed no downregulation of miR-150 of her NK cells obtained from her peripheral blood, despite the CD56$^+$ phenotype of the tumor (Figure 2b). Figure 2c shows two cases of NK-cell lymphoma, extranodal type, representing very low expression of miR-150 when compared with normal NK cells.

Transduction of miR-150 into lymphoma lines and % GFP monitoring

To determine the role of miR-150 in the tumorigenesis of NK/T-cell lymphomas, we transduced miR-150 along with GFP into five NK/T-cell lymphoma cell lines (YT, KAI-3, MOTN-1, SNK-6 and HANK-1) and two B-cell lymphoma cell lines (Raji and Daudi). The transduction efficiencies were as follows: YT,

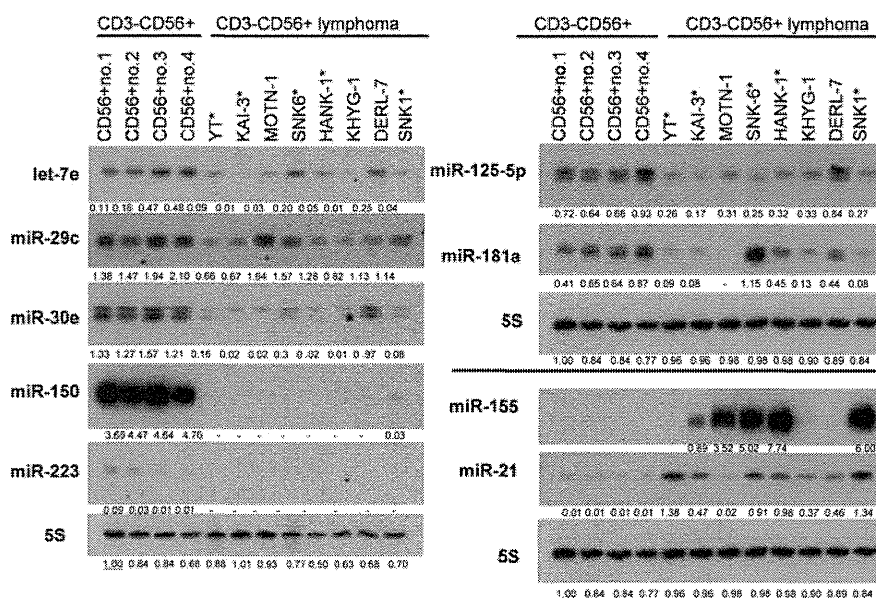

Figure 1 Expression analysis of downregulated miRNAs in NK/T-cell lymphoma/leukemia lines. Northern analysis of the expression of the indicated miRNAs in eight NK-cell lymphoma cell lines (sCD3$^-$CD56$^+$) and four samples of normal (sCD3$^-$CD56$^+$) NK cells. The cell types are indicated at the top. Fold changes in miRNA levels were determined by densitometry and are shown below the gels after normalization to the level of 5S RNA in normal NK cells (number 1), which was assigned a value of 1.00. Controls (5S tRNA) are shown below the miR-34a and miR-15a blots, respectively. Asterisks (*) indicate cell lines showing Epstein–Barr virus infection.

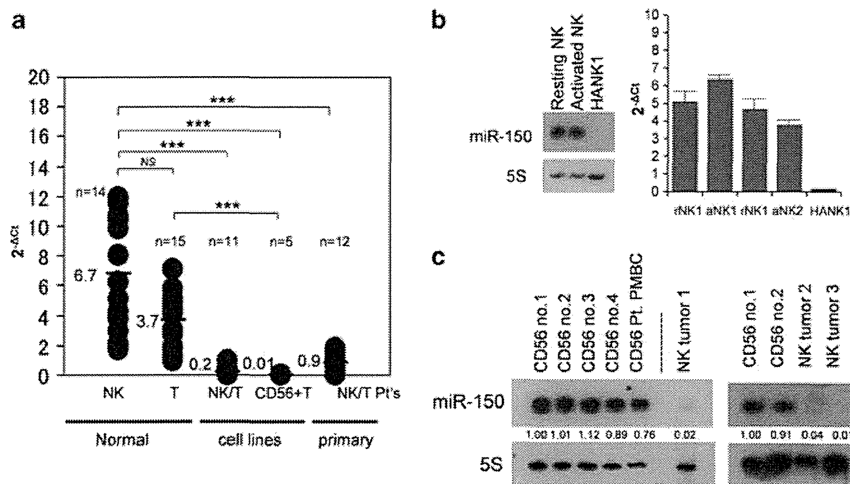

Figure 2 miR-150 expression in primary NK/T-cell lymphoma/leukemia cases. (**a**) Quantitative PCR analysis of miR-150 expression in sCD3$^-$CD56$^+$ NK cells (NK, $n=14$), sCD3$^+$ T-cells (T, $n=15$), NK-cell lymphoma lines (NK/T, $n=11$), CD56$^+$ T-cell lymphoma lines (CD56$^+$T, $n=5$) and primary NK/T-cell tumor samples (NK/T patients, $n=12$). The horizontal lines indicate the means. *y* axis, $-\Delta Ct$ values for miRNA expression. Statistical significance: NS, not significant, ***$P<0.001$. (**b**) miR-150 expression in resting and activating NK cells. Left panel, Northern blot. Right panel, Taqman PCR. rNK, resting NK. aNK, activated NK. (**c**) Left panel, Northern blot analysis of miR-150 expression in normal resting NK cells (rNK number 1–4, $n=4$), NK cell of a patient and a samples from the patient with NK/T-cell lymphoma, nasal type (described as NK tumor 1). Right panel, Northern blot analysis of miR-150 expression in NK cells ($n=2$) and two patients with NK/T-cell lymphoma, nasal type (NK tumors 2 and 3), whose RNA was also purified from CD56$^+$ cells.

2.1%; KAI-3, 3.4%; HANK-1, 5.8%; SNK-6, 6.5%; MOTN-1, 9.7%; Raji, 3.5%; and Daudi, 3.75%. At 14 days later, RNA from the transductants was collected, based on GFP selection (day 0), and subjected to Northern analysis, which showed upregulation of GFP-miR-150 with no changes in the expression of miR-21 or miR-155, as compared with cells transduced with GFP alone (Figure 3a). Quantitative PCR also showed upregulation of miR-150 in all transduced cell lines (Figure 3b). Expressions of miR-150 of all cell lines between normal and GFP$^+$ vector-transduced cells showed no differences in the expressions (data not shown).

After initially monitoring % GFP among cells in culture, the conditions for lentiviral infection were adjusted to achieve ~50% GFP-miR-150 positivity among recipient cells (1:1 mixture of ~100% GFP$^+$ cells and GFP$^-$ cells), after which the mixed cultures were monitored weekly using a flow cytometer. Figure 3c shows the changes in %GFP-miR-150 among HANK-1 cells from day 7 to day 28 after GFP-miR-150 selection. We observed a reduction in %GFP-miR-150 beginning at 14 days after GFP-miR-150 selection, which might have been caused by displacement of GFP$^-$ cells. As shown in Figure 3d, a reduction in %GFP-miR-150 was seen in the YT, MOTN-1, HANK-1 and SNK-6 lines, but not in KAI-3 cells or in the two B-cell lymphoma lines, whereas the cell lines transduced with GFP vector did not show the reduction in any cell lines examined. Transduced SNK-6 cells showed a slight upregulation of miR-150 when compared with other transduced cell lines. This effect might be linked to a lower 'decreasing rate (75–80%)' than was seen with the other transduced cells such as MOTN-1 and HANK-1.

miR-150 increases susceptibility to apoptosis and reduces cell proliferation in NK/T-cell lymphoma cell lines

To detect the function of miR-150 during tumorigenesis, we assessed the incidence of apoptosis among transduced cells following exposure to etoposide (100 μM for 4 h) on day 14 after selection. We found that the incidence of apoptosis in the presence of etoposide was increased in MOTN-1 cells (Figure 4a). When we then carried out 5′-bromo-2′-deoxyuridine assays with MOTN-1 cells, we found that the 5′-bromo-2′-deoxyuridine index was significantly reduced in cells transduced with miR-150 (Figure 4b). The same results were obtained in HANK-1 cells (Figures 4c and d). Although SNK-6 cells did not show increased apoptosis when transduced with miR-150 alone, greater numbers of apoptotic cells were detected when the miR-150 was transduced into miR-155 knockdown cells (Figure 5). Similarly, miR-150-positive MOTN-1 and HANK-1 cells expressing ASO-155 did not show a significant increase in the incidence of apoptosis (Supplementary Figure 3). In addition, apoptosis assays with YT cells revealed a cooperative effect between miR-21 and miR-150. YT cells transduced with miR-150 showed significantly larger numbers of apoptotic cells if they were treated with ASO-21 (Figure 5). Moreover, combining miR-150 transduction with miR-21 knockdown induced significant increases in the incidence of apoptosis. In addition, when we carried out 5′-bromo-2′-deoxyuridine assays with SNK-6 and YT cells, we found that the 5′-bromo-2′-deoxyuridine index was significantly reduced in these cells transduced with miR-150 without additive effects (data not shown).

miR-150, thus, appears to function as a tumor suppressor by increasing cell susceptibility to apoptosis and decreasing cell cycle progression, although the effect does not induce a marked reduction in % GFP.

miR-150 induces senescence in NK/T-cell lymphoma lines

We speculated that the reduction in %GFP among miR-150 transductants during culture might reflect cellular senescence. To test this idea, we transduced miR-150 into cells from the YT, MOTN-1, SNK-6 and HANK-1 lines, which had previously showed reductions in %GFP during culture (Figure 3). The miR-150 transduction efficiency was about 5–10%, which was

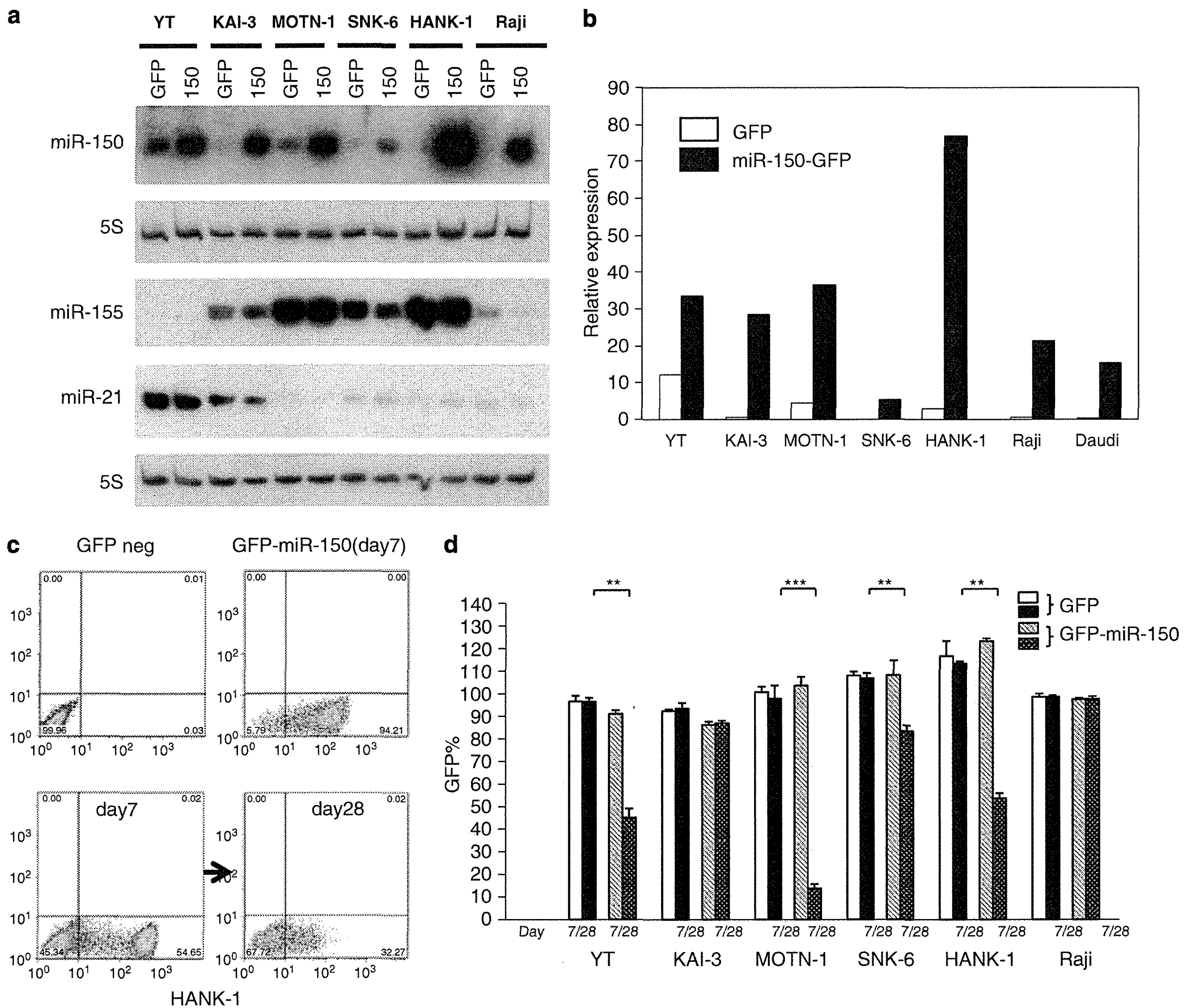

Figure 3 Transduction of miR-150 in lymphoma lines and GFP% monitoring. (**a**) Northern blot analysis of the indicated miRNAs in cells transduced with miR-150 or empty vector (GFP$^+$). The transductant cell type is indicated at the top. Controls (5S tRNA) are shown in the bottom panel. (**b**) Quantitative PCR analysis of miR-150 expression in the indicated cell types transduced with empty vector or miR-150. *y* axis: black and white bars depict $-\Delta Ct$ values for miR-150 expression. *x* axis: cell lines transduced with empty vector (GFP) or miR-150. (**c**) Flow cytometric analysis of the GFP$^+$ fraction (%GFP) among transduced HANK-1 cells. Upper panels: left, GFP$^-$ cells; right, cells transduced with miR-150-GFP (%GFP = approximately 100). Lower panels: left, GFP-miR-150 on day 7 (%GFP = approximately 50); right panel, GFP-miR-150 on day 28. Days: days after GFP-miR-150 selection; alternatively day 0 is at 48 h after GFP-miR-150 transduction. (**d**) %GFP among NK/T-cell lymphoma (YT, KAI-3, MOTN-1, SNK-6 and HANK-1) and Burkitt lymphoma (Raji) lines transduced with GFP-miR-150 or empty vector (GFP). White bars indicate %GFP for GFP transductants on day 7 after GFP selection; black bars, the %GFP for GFP transductants on day 28. Gray bars show the %GFP for GFP-miR-150 transductants on day 7; dark gray bars, the %GFP for GFP-miR-150 transductants on day 28 (YT, MOTN-1, SNK-6 and HANK-1) or day 42 (KAI-3 and Raji). Statistical significance: $^{**}P<0.01$ and $^{***}P<0.001$.

the same as in earlier experiments. After the transduction, GFP$^+$ cells were selected in a cell sorter. We found that the rate of growth of MOTN-1, SNK-6 and HANK-1 cells transduced with miR-150 was lower among cells transduced with empty vector (data of MOTN-1 and HANK-1 are shown in Figure 6a). In addition, these cells stained positively for Ki-67 and senescence-associated beta-gal on day 21 after GFP selection and miR-150 transductants had a 'fried egg'-like appearance, which is caused by senescence and is not seen in normal NK/T-cell lymphoma cells (data of HANK-1 are shown in Figure 6b).

We also used telomeric repeat amplification protocol assays to assess telomerase activity in MOTN-1, SNK-6 and HANK-1 cells, with and without miR-150 transduction, and in normal NK cells. We found that resting and activated NK cells showed no telomerase activity (Figure 6c), whereas NK/T-cell lymphoma cell lines did so, indicating a reverse correlation between expression of miR-150 and telomerase activity (Figure 6c). As shown in Figure 6d, telomerase activity in miR-150 transductants (on day 21 after GFP selection) was markedly lower than in cells transduced with empty vector. Because it is known that lymphocytes without telomerase activity show telomeric DNA shortening during cell culture,[22] we used Southern blot analysis to assess the telomere length in HANK-1, MOTN-1 and SNK-6 cells. Genomic DNA was digested by *Hin*fI, which does not cleave within the repeating (TTAGGG)n sequence that constitutes the telemetric DNA. The lengths of the resultant telemetric

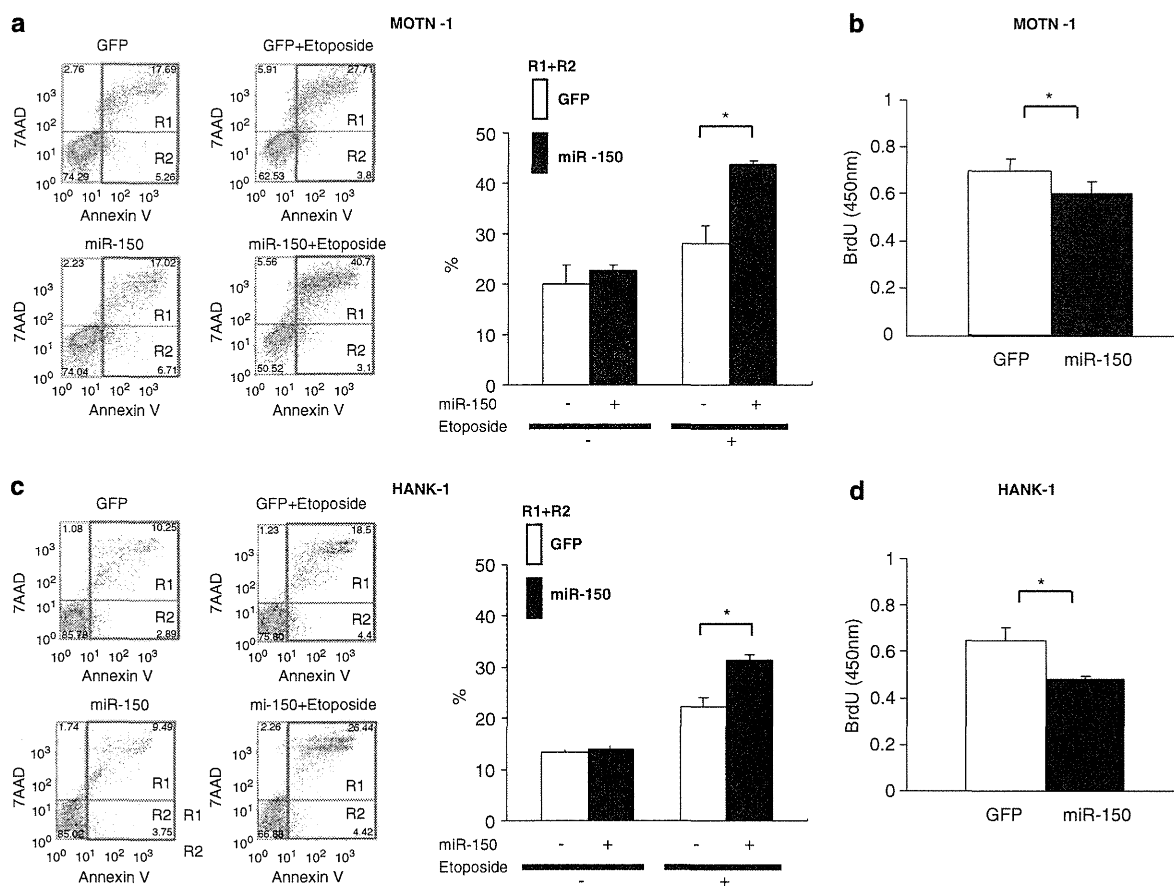

Figure 4 Assays of apoptosis and cell proliferation in miR-150-transduced NK/T-cell lymphoma lines. (**a**) Apoptosis among MOTN-1 cells transduced with miR-150 or empty vector (GFP$^+$). miR-150 transductants were exposed to 100 μM etoposide for 4 h. Left panels: flow cytometric analysis of miR-150 transductants: *y* axis, cells stained by 7-AAD; *x* axis, cells stained by Annexin V-PE. Right panel: Percentages of apoptotic cells (R1 + R2). White and black bars depict percent apoptosis (R1 + R2) among MOTN-1 cell transduced with miR-150. (**b**) Cell proliferation assays (5′-bromo-2′-deoxyuridine assay) in MOTN-1 cells. The white bar shows the 5′-bromo-2′-deoxyuridine index (450 nm) for GFP transductants; the black bar, the 5′-bromo-2′-deoxyuridine index for GFP-miR-150 transductants. (**c**) Apoptosis assays in HANK-1 cells transduced with miR-150 or empty vector (GFP$^+$). (**d**) Cell proliferation assays (5′-bromo-2′-deoxyuridine assay) in HANK-1 cells. The white bar shows the 5′-bromo-2′-deoxyuridine index for GFP transductants; the black bar, the 5′-bromo-2′-deoxyuridine index for GFP-miR-150 transductants. Statistical significance: *$P<0.05$.

restriction fragments were then determined by gel electrophoresis followed by Southern analysis using a probe that recognizes this sequence. As shown in Figure 6e, we observed a shortening of telomeric DNA in the cells expressing miR-150 during continuous culture. Indeed, the telemetric restriction fragments of miR-150 transductants grew shorter with every successive passage (Figure 6f). Thus, miR-150 appears to control aging and senescence in mature lymphocytes.

Identification of direct targets of miR-150 and the downstream targets in NK/T-cell lymphoma

We used Target Scan (http://www.targetscan.org) and Pigtar (http://pictar.mdc-berlin.de) to predict miR-150 targets.[23,24] We then used western analysis to assess expression in various candidate targets, including c-Myb,[25] FOXP1,[26] BCAP (*PIK3AP1*), p85 (*PIK3R1*), AKT2, AKT3, PRL1, Pim1, RECK, Rictor, c-Raf, MSK1, MIB1, ELK1, E2F3 and MLL in MOTN-1, SNK-6 and HANK-1 cells transduced with miR-150 or empty vector. These proteins include upstream mediators of signal transduction, such as AKT, STAT3 and Ras, and might be associated with tumorigenesis when downregulated by forced expression of miR-150. We also analyzed expression of the telomerase-related proteins Dyskerin (gene name dyskeratosis congenita 1, *DKC1*), SirT1, PAI-1, Mre1 and ERCC1, which also possess seed sequences (but not conserved) of miR-150. Of these, loss of Dyskerin function is known to induce senescence.[27] We found that levels of both AKT2 and Dyskerin were reduced in all miR-150 transductants (Figure 7a), whereas BCAP expression was slightly reduced in SNK-6 and HANK-1 cells (data not shown). To determine whether these proteins are direct targets of miR-150, we carried out luciferase reporter assays in Rat-1 fibroblasts stably expressing miR-150. Upon insertion of the wild-type 3′-UTR of *DKC1, PIK3AP1, AKT3* or *AKT2* into the reporter, we observed significant reductions in luciferase activity with *DKC1, PIK3AP1* and *AKT2*, but not in *AKT3* (data not shown), as compared with cells transduced with empty vector (control vector), suggesting that *DKC1, PIK3AP1* (data not shown) and *AKT2* have potential to function as direct targets of miR-150 (Figure 7b).

Overexpression of AKT2 with upregulation of pAKT^{ser474}, which enhances telomerase activity through phosphorylation of human telomerase reverse transcript (hTERT), has been observed in various cancers.[28,29] We therefore carried out a western analysis of pAKT$^{ser473/4}$ expression and found it to be markedly reduced in the cells tested. We also detected upregulation of

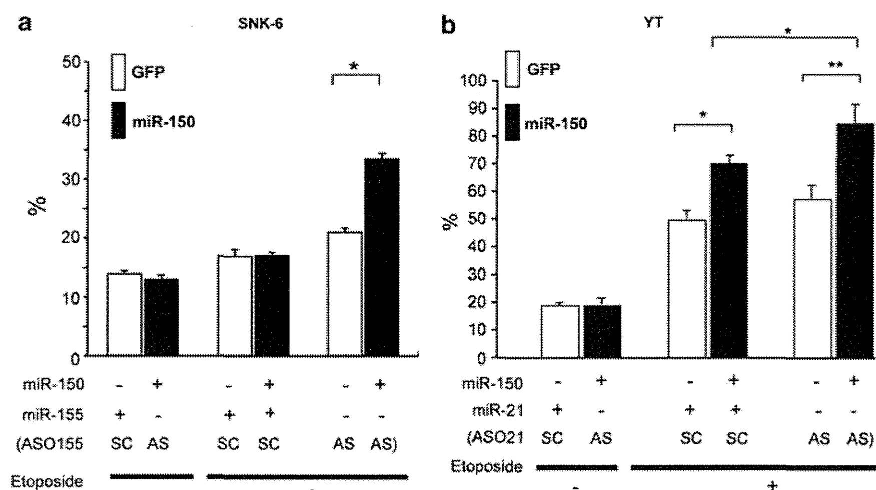

Figure 5 Cooperative effects of miRNAs enhance apoptosis. (**a**) Apoptosis assays in SNK-6 cells transduced with miR-150 or empty vector (GFP^+). Left panel: apoptosis assay. (+) and (−) indicate the presence (+) or absence (−) of miR-155 or miR-150 expressions. ASO-155: cells treated with antisense mR-155 oligo. SC: scramble. AS: antisense. Symbols and bars indicate means and s.d.'s of triplicate samples. Statistical significance: NS, not significant, $*P<0.05$. (**b**) Percentages of apoptotic cells. White and black bars depict percent apoptosis among YT cells transduced with miR-150. (+) and (−) indicate the presence (+) or absence (−) of miR-21 or miR-150 expressions. YT cells show overexpression of miR-21 without expression of miR-155 or miR-150. ASO-21: cells treated with antisense mR-21 oligo. SC: scramble. AS: antisense. Statistical significance: NS, not significant, $*P<0.05$ and $**P<0.01$.

Bim (in MOTN-1, HANK-1 and SNK-6) and p53 (in SNK-6 and HANK-1) (Figure 7c). Bim is a BH3 proapoptotic protein and its upregulation can lead to apoptosis.[30] Upregulation of these tumor suppressors might be linked to pAKT downregulation, although further study will be needed to determine whether or not these changes in expression are pAKT-dependent.

Discussion

Recent studies have shown deregulations of coding genes in NK/T-cell lymphoma.[14,31,32] However, there are no reports of miRNA deregulations in these subtypes. In this study, we assessed miR-150 expression in NK cell and $CD56^+$ T-cell lymphomas, and found it to be significantly reduced. Although aberrantly low expression of miR-150 has been identified in Sezary syndrome,[33] which is classified as a T-cell lymphoma, there have been no reports on its expression and function during NK/T-cell lymphomagenesis. Almost none of the tested cell lines and primary samples of NK/T-cell lymphoma showed expression of miR-150, though mature T and NK cells normally expressed high levels of miR-150,[34] suggesting downregulation miR-150 in lymphomas might be important for lymphomagenesis and contribute to immortalization of the cancer cells. It is also known that normal lymphocytes show senescence with increasing population doublings.[22] Our results suggest that the continuous expression of miR-150 in normal mature lymphocytes may be required to prevent immortalization, which may be a first step toward developing cancer.

Our findings also suggest that downregulation of miR-150 can lead to activation of telomerase via upregulation of AKT2, a prosurvival protein serine/threonine kinase activated via the PI3K pathway, which is a key prosurvival pathway in cancer.[28,29,35–39] Several studies have shown that *AKT2* gene is overexpressed in various tumor cell lines and human malignancies, including B-cell lymphoma, liver, ovarian, pancreatic and breast cancers; and that overexpression of AKT2 protein is associated with increased invasion and metastasis.[35–39] Thus, AKT2 appears to have a crucial role in tumorigenesis.

Activation of the PI3K–AKT pathway through phosphorylation of Serine 474 in AKT2 is strongly associated with tumorigenesis. For example, $pAKT^{ser473/4}$ can upregulate telomerase via phosphorylation of hTERT, resulting in immortalization of cancer cells. Kang *et al*[40] reported that the hTERT subunit has two AKT kinase phosphorylation sites (Ser473 and Thr308 in AKT1/AKT3, Ser474 and Thr309 in AKT2) and that pAKT contributes to telomerase activity through phosphorylation of hTERT. Conversely, inhibition of PI3K–AKT signaling reduces telomerase activity. For example, Plunkett *et al.*[41] reported that, in T cells, the loss of telomerase activity is associated with reduced levels of $pAKT^{ser473/4}$. It is also known that inhibition of AKT signaling by p27 induces a senescence-like arrest, independent of p53.[42] Consistent with those reports, our results strongly suggest that activation (phosphorylation) of AKT due to the loss of miR-150 expression may have a key role in enhancing human telomerase activity in the cancer cells.

Interestingly, forced expression of miR-150 can also lead to downregulation of *DKC1*/Dyekerin *in* NK/T-cell lymphoma cells, suggesting that loss of miR-150 may activate Dyskerin. It is encoded by *DKC1* and is a predominantly nucleolar protein essential for the formation of pseudouridine in RNA and the telomerase RNA subunit hTR.[43,44] Dyskeratosis congenita patients have a nonsense mutation within *DKC1*, leading to diminished expression of Dyskerin accompanied by downregulation of telomerase activity.[45] Overexpression of *DKC1* has been seen in solid tumors, and the silencing of *DKC1* can reduce telomerase activity and rRNA pseudouridylation.[46,47] These findings suggest that the level of Dyskerin expression parallels the activation and inactivation of telomerase. Together, activation of hTERT via pAKT and the continuous expression of Dyskerin could contribute to the enhancement of telomerase activity; however, it is still unclear whether the reduced expression of Dyskerin leads directly to inactivation of telomerase or whether telomerase is regulated via miR-150 itself.

In the present study, we do not address the mechanism underlying the loss of miR-150 expression in NK/T-cell

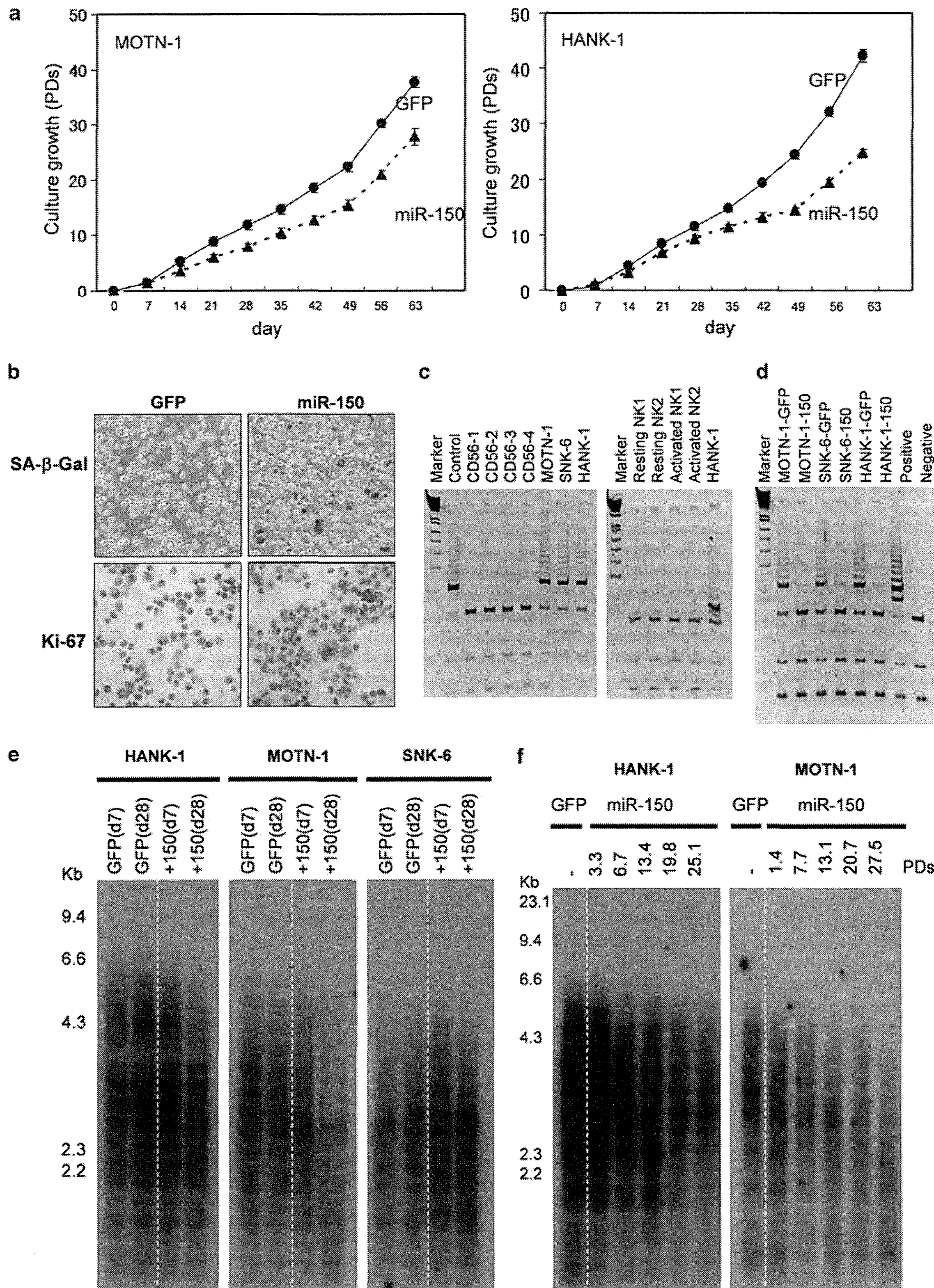

Figure 6 miR-150 induces senescence in NK/T-cell lymphoma lines. (**a**) Cell growth assay in MOTN-1 and MOTN-1 cells. PDs, population doublings. Days, days after GFP-miR-150 selection; alternatively day 0 is at 48 h after GFP-miR-150 transduction. (**b**) Senescence assay in HANK-1 cells. Upper panels: senescence-associated beta-gal assay. Lower panels: Ki-67 staining of HANK-1 cells transduced with empty vector (GFP) or miR-150. (**c**) Telomerase activity in NK cells and NK-cell lymphoma lines. Left panel: telomeric repeat amplification protocol assay with normal NK-cells (four samples) and NK-cell lymphoma lines (MOTN-1, SNK-6 and HANK-1). Right panel: telomeric repeat amplification protocol assay with resting (rNK) and activated NK cells (aNK) and HANK-1 cells. (**d**) Telomerase activity (TRAP assay) in NK cells transduced with empty vector (GFP) or miR-150. (**e**) Southern blot analysis of HANK-1, MOTN-1 and SNK-6 cell lines, with (day 7) and without (day 28) miR-150 expression. (**f**) Changes in telomere length in HANK-1 and MOTN-1 cells with PDs. GFP, cells transduced with empty vector. miR-150, NK-cell lymphoma cells transduced with miR-150.

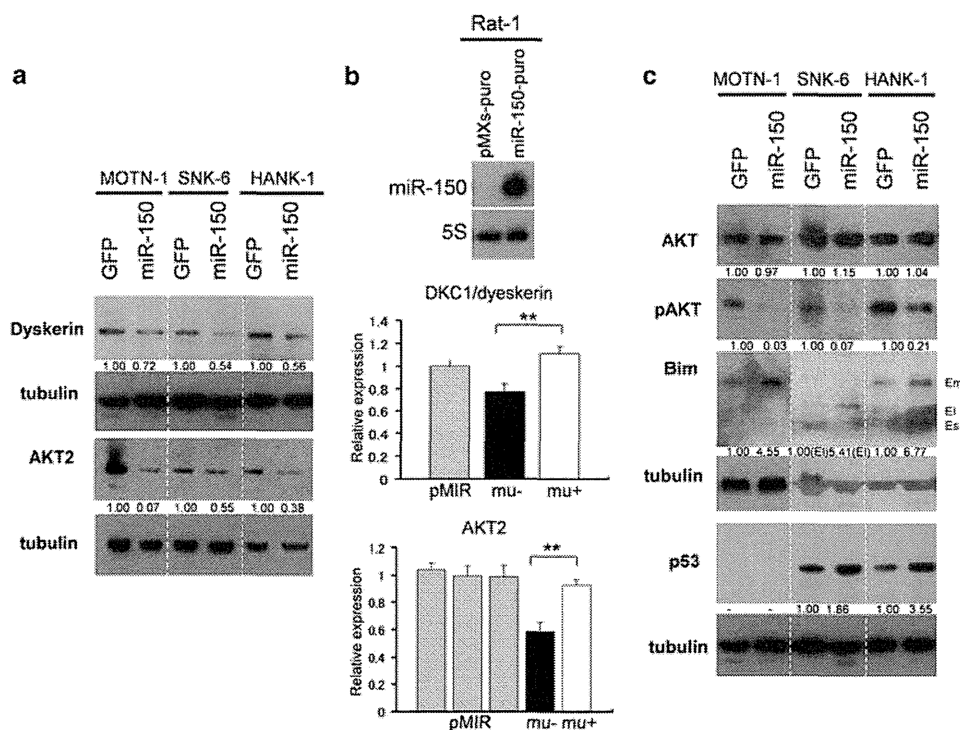

Figure 7 Luciferase assay of miR-150 targets and the expression of downstream AKT. (**a**) Western blot analysis of Dyskerin (*DKC1*) and AKT2 expression in MOTN-1, SNK-6 and HANK-1 cells in the presence or absence of miR-150 expression. (**b**) Luciferase reporter assays of *AKT2* and *DKC1* expression in Rat-1 cells transfected with miR-150 or empty vector (pMIR). Blots showing miR-150 expression are beside the bars. Statistical significance: NS, not significant, $^{**}P<0.01$. (**c**) Western analysis of $\text{pAKT}^{\text{ser473/4}}$ expression and expression of its downstream targets. MOTN-1, SNK-6 and HANK-1 cells transduced without (GFP) and with miR-150 are lined. Examined downstream proteins are Bim and p53. Fold changes in protein levels are shown below the gels and are normalized to the level in the respective miR-150-transduced cell lines, which were assigned a value of 1.00.

lymphomas. We can say, however, that it is likely not the result of genomic alteration and/or an epigenetic mechanism, such as deletion or methylation/deacetylation. Fluorescence *in situ* hybridization analysis of 19q31.33 in all eleven NK/T-cell lymphoma cell lines revealed no genomic deletion, and 5-Aza-2′-deoxycydine (a DNA methyltransferase inhibitor) and/or trichostatin A (a histone deacetylase inhibitor) did not restore miR-150 activity in these lymphoma cells (data not shown). Previously, Chang *et al.*[48] showed that miR-150 is downregulated by c-Myc and that miR-150 may function as a tumor suppressor, asw injection of mouse lymphoma cell lines into mice expressing miR-150 produced fewer tumor cells *in vivo*. We used Northern and western blot analyses to examine c-Myc expression in NK (YT, KAI-3, MOTN-1, SNK-6 and HANK-1) and B-cell (Raji and Daudi) lymphoma lines (these cell lines showed no expression of miR-150). Although the B-cell lymphoma lines strongly expressed c-Myc, two (KAI-3, and YT) of the five NK-cell lymphoma lines did not express c-Myc (Supplementary Figure 4). Given that these two cell lines also did not express miR-150, it is not likely that the downregulation of miR-150 was due to c-Myc, at least not in these cells. This suggests there is another regulator of miR-150.

We previously demonstrated that miR-21 and/or miR-155 are overexpressed in NK-cell lymphomas.[13] These miRNAs, respectively, downregulate the phosphatases PTEN and SHIP1, leading to activation of the PI3K–AKT pathway. In earlier studies[13] and the present one, we found that miR-21 could function as an oncomiR by enhancing anti-apoptotic activity in NK-cell tumors, and that the effect was strengthened when miR-21 functioned cooperatively with miR-150. Our findings also indicate that transduction of miR-155 alone did not increase oncogenic activity, despite a slight upregulation of pAKT. However, our observation that knockdown of miR-155 alone increased the incidence of apoptosis cells when it was expressed with miR-150 suggests that miR-155 may serve as an oncomiR, though its activity is weaker than that of miR-21 or miR-150. This suggests miR-155 may function as an enhancer of oncomiRs in NK cell tumors. Our earlier findings showed that expression of miR-21 and miR-155 is mutually exclusive in both NK cell lines and primary tumors from patients.[13] In the present study, we found that miR-150 is downregulated in both NK cell lines and primary tumors. These oncomiRs may function cooperatively to enable the continuous activation of PI3K–AKT signaling, ultimately leading to enhancing anti-apoptotic activity, cell cycle progression, cell proliferation and immortalization via targeting of downstream mediators such as hTERT, p53 and Bim.

In summary, we have shown that miR-150 functions as a tumor suppressor in NK/T-cell lymphomas. Our results also suggest that miR-150 likely serves as an upstream regulator of the PI3K–AKT pathway. These findings could provide a basis for new therapies targeting AKT in the treatment of NK/T-cell lymphoma.

Conflict of interest

The authors declare no conflict of interest.

Acknowledgements

This work is supported in by a Grant-in-Aid from the Japan Society for the Promotion of Science (HT). We wish to express our appreciation to Ms E Kobayashi, Y Abe, Y Chiba and H Kataho for their outstanding technical assistance, Dr T Nanjo (Akita University, Akita, Japan) and Dr R Ichinohasama (Tohoku University,
Sendai, Japan) for their histological and/or clinical diagnosis of lymphoma. Antibody against BCAP was kindly provided from Professor T Kurosaki (RIKEN). pMX vector was kindly provided by Dr T Kitamura (Tokyo University, Tokyo, Japan).

Author contributions

AW performed all experiments, analyzed data, designed experiments and constructed figures and tables. HT designed and performed experiments, analyzed data, wrote the paper and organized the study. JY, KT, MN, KI, MK, YK, NT, TN, SN and KS performed experiments and analyzed data.

References

1 Jaffe ES, Harris NL, Stein H, Campo E, Pileri SA, Swerdlow SH. Introduction and over review of the classification of the lymphoid neoplasms. In: Swerdloe, A.H., Campo E, Harris NL, Jaffe ES, Stein H, Thiele J, Vardiman JW (eds). *World Health Organization Classification of Tumors of Haematopoietic and Lymphoid Tissues*. IARC press: Lyon, Washington, 2008, pp 158–178.
2 Siu LL, Wong KF, Chan TK, Kwong YL. Comparative genomic hybridization analysis of natural killer cell lymphoma. *Am J Pathol* 1999; **155**: 1419–1425.
3 Siu LLP, Chan V, Chan JKC, Wong KF, Liang R, Kwong YL. Consistent patterns of allelic loss in natural killer cell lymphoma. *Am J Pathol* 2000; **157**: 1803–1809.
4 Wong KF, Zhang YM, Chan JK. Cytogenetic abnormalities in natural killer cell lymphoma/leukemia: is there a consistent pattern? *Leuk Lymphoma* 1999; **34**: 241–250.
5 Yoon J, Ko YH. Deletion mapping of the long arm of chromosome 6 in peripheral T and NK cell lymphomas. *Leuk Lymphoma* 2003; **44**: 2077–2082.
6 Ko YH, Choi KE, Han JH, Kim JM, Ree HJ. Comparative genomic hybridization study of nasal-type NK/T-cell lymphoma. *Cytometry* 2001; **46**: 85–91.
7 Nakashima Y, Tagawa H, Suzuki R, Karnan S, Karube K, Ohshima K *et al.* Genome-wide array-based comparative genomic hybridization of natural killer cell lymphoma/leukemia: different genomic alteration patterns of aggressive NK-cell leukemia and extranodal NK/T cell lymphoma, nasal type. *Genes Chromosomes Cancer* 2005; **44**: 247–255.
8 Iqbal J, Kucuk C, Deleeuw RJ, Srivastava G, Tam W, Geng H *et al.* Genomic analyses reveal global functional alterations that promote tumor growth and novel tumor suppressor genes in natural killer-cell malignancies. *Leukemia* 2009; **23**: 1139–1151.
9 Bartel DP. MicroRNAs: genomics, biogenesis, mechanism, and function. *Cell* 2004; **116**: 281–297.
10 Iorio MV, Croce CM. MicroRNAs in cancer: small molecules with a huge impact. *J Clin Oncol* 2009; **27**: 5848–5856.
11 Croce CM. Causes and consequences of microRNA dysregulation in cancer. *Nat Rev Genet* 2009; **10**: 704–714.
12 Esquela-Kerscher A, Slack FJ. Oncomirs-microRNAs with a role in cancer. *Nat Rev Cancer* 2006; **6**: 259–269.
13 Yamanaka Y, Tagawa H, Takahashi N, Watanabe A, Guo Y-M, Iwamoto K *et al.* Aberrant overexpression of microRNAs activate AKT signaling via down-regulation of tumor suppressors in natural killer-cell lymphoma/leukemia. *Blood* 2009; **114**: 3265–3275.
14 Huang Y, de Reynies A, de Leval L, Ghazi B, Martin-Garcia N, Travert M *et al.* Gene expression profiling identifies emerging oncogenic pathways operating in extranodal NK/T-cell lymphoma, nasal type. *Blood* 2010; **115**: 1226–1237.
15 Kagami Y, Nakamura S, Suzuki R, Iida S, Yatabe Y, Okada Y *et al.* Establishment of an IL-2-dependent cell line derived from 'nasal-type' NK/T-cell lymphoma of CD2+, sCD3-, CD3e+, CD56+ phenotype and associated with the Epstein-Barr virus. *Br J Haematol* 1998; **103**: 669–677.
16 Nagata H, Konno A, Kimura N, Zhang Y, Kimura M, Demachi A *et al.* Characterization of novel natural killer (NK)-cell and gamma delta T cell lines established from primary lesions of nasal T/NK cell lymphomas associated with the Epstein-Barr virus. *Blood* 2001; **97**: 708–713.
17 Matsuo Y, Drexler HG, Takeuchi M, Tanaka M, Orita K. Establishment of the T-cell large granular lymphocyte leukemia cell line MOTN-1 carrying natural killer-cell antigens. *Leukemia Res* 2002; **26**: 873–879.
18 Zhang Y, Nagata H, Ikeuchi T, Mukai H, Oyoshi MK, Demachi A *et al.* Common cytological and cytogenetic features of Epstein-Barr virus (EBV)-positive natural killer (NK) cells and cell lines derived from patients with nasal T/NK-cell lymphomas, chronic active EBV infection and hydroa vacciniforme-like eruptions. *Br J Haematol* 2003; **121**: 805–814.
19 Inomata M, Tagawa H, Guo YM, Kameoka Y, Takahashi N, Sawada K. MicroRNA-17–92 down regulates expression of distinct targets in different B-cell lymphoma subtypes. *Blood* 2009; **113**: 396–402.
20 Chen C-Z, Li L, Lodish HF, Bartel DP. MicroRNA modulate hematopoietic linage differentiation. *Science* 2004; **303**: 83–86.
21 Merkerova M, Belickova M, Brucova H. Differential expression of microRNAs in hematopoietic cell linages. *Eur J Haematol* 2008; **81**: 304–310.
22 Counter CM, Botelho FM, Wang P, Harley CB, Bacchetti S. Stabilization of short telomeres and telomerase activity accompany immortalization of Epstein-Barr virus-transformed human B lymphocytes. *J Virol* 1994; **68**: 3410–3414.
23 Lewis BP, Shih IH, Rhoades MW, Bartel DP, Burge CB. Prediction of mammalian microRNA targets. *Cell* 2003; **115**: 787–798.
24 Krek A, Grün D, Poy MN, Wolf R, Rosenberg L, Epstein EJ *et al.* Combinational microRNA target predictions. *Nat Genet* 2005; **37**: 495–500.
25 Xiao C, Calado DP, Galler G, Thai TH, Patterson HC, Wang J *et al.* MiR-150 controls B cell differentiation by targeting the transcription factor c-Myb. *Cell* 2007; **131**: 146–159.
26 Tan LP, Wang M, Robertus JL, Schakel RN, Gibcus JH, Diepstra A *et al.* miRNA profiling of B-cell subsets: specific miRNA profile for germinal center B cells with variation between centroblasts and centrocytes. *Lab Invest* 2009; **89**: 708–716.
27 Mitchell JR, Wood E, Collins K. A telomerase component is defective in the human disease dyskeratosis congenita. *Nature* 1999; **402**: 551–555.
28 Testa JR, Bellacosa A. AKT plays a central role in tumorigenesis. *Proc Natl Acad Sci USA* 2001; **98**: 10983–10985.
29 Vivanco I, Sawyers CL. The phosphatidylinositol 3-kinase AKT pathway in human cancer. *Nat Rev Cancer* 2002; **2**: 489–501.
30 O'Connor L, Strasser A, O'Reilly LA, Hausmann G, Adams JM, Cory S *et al.* Bim: a novel member of the Bcl-2 family that promotes apoptosis. *EMBO J* 1998; **17**: 384–395.
31 Iqbal J, Weisenburger DD, Chowdhury A, Tsai MY, Srivastava G, Greiner TC *et al.* Natural killer cell lymphoma shares strikingly similar molecular features with a group of non-hepatosplenic $\gamma\delta$ T-cell lymphoma and is highly sensitive to a novel aurora kinase A inhibitor *in vitro*. *Leukemia* 2011; **25**: 348–358.
32 Ng SB, Selvarajan V, Huang G, Zhou J, Feldman AL, Law M *et al.* Activated oncogenic pathways and therapeutic targets in extranodal nasal-type NK/T cell lymphoma revealed by gene expression profiling. *J Pathol* 2011; **223**: 496–510.
33 Ballabio E, Mitchell T, van Kester MS, Taylor S, Dunlop HM, Chi J *et al.* MicroRNA expression in Sezary syndrome: identification, function, and diagnostic potential. *Blood* 2010; **116**: 1105–1113.
34 Zhou B, Wang S, Mayr C, Bartel DP, Lodish HF. miR-150, a microRNA expressed in mature B and T cells, blocks early B cell development when expressed prematurely. *Proc Natl Acad Sci USA* 2007; **104**: 7080–7085.
35 Arranz E, Robledo M, Martinez B, Gallego J, Roman A, Rivas C *et al.* Incidence of homogeneously staining regions in non-Hodgkin lymphomas. *Cancer Genet Cytogenet* 1996; **87**: 1–3.

36 Xu X, Sakon M, Nagano H, Hiraoka N, Yamamoto H, Hayashi N *et al.* Akt2 expression correlates with prognosis of human hepatocellular carcinoma. *Oncol Rep* 2004; **11**: 25–32.
37 Thompson FH, Nelson MA, Trent JM, Guan XY, Liu Y, Yang JM *et al.* Amplification of 19q13.1-q13.2 sequences in ovarian cancer. G-band, FISH, and molecular studies. *Cancer Genet Cytogenet* 1996; **87**: 55–62.
38 Cheng JQ, Ruggeri B, Klein WM, Sonoda G, Altomare DA, Watson DK *et al.* Amplification of AKT2 in human pancreatic cells and inhibition of AKT2 expression and tumorigenicity by antisense RNA. *Proc Natl Acad Sci USA* 1996; **93**: 3636–3641.
39 Arboleda MJ, Lyons JF, Kabbinavar FF, Bray MR, Snow BE, Ayala R *et al.* Overexpression of AKT2/protein kinase B beta leads to up-regulation of beta1 integrins, increased invasion, and metastasis of human breast and ovarian cancer cells. *Cancer Res* 2003; **63**: 196–206.
40 Kang SS, Kwon T, Kwon DY, Do SI. Akt protein kinase enhances human telomerase activity through phosphorylation of telomerase reverse transcriptase subunit. *J Biol Chem* 1999; **274**: 13085–13090.
41 Plunkett FJ, Franzese O, Finney HM, Fletcher JM, Belaramani LL, Salmon M *et al.* The loss of telomerase activity in highly differentiated CD8+CD28-CD27-T cells is associated with decreased Akt (Ser473) phosphorylation. *J Immunol* 2007; **178**: 7710–7719.
42 Collado M, Medema RH, Garcia-Cao I, Dubuisson HLN, Barradas M, Glassford J *et al.* Inhibition of the phosphoinositide 3-kinase pathway induces a senescence-like arrest mediated by p27Kip1. *J Biol Chem* 2002; **275**: 21960–21968.
43 Heiss NS, Knight SW, Vulliamy TJ, Klauck SM, Wiemann S, Mason SPJ *et al.* X-linked dyskeratosis congenita is caused by mutations in a highly conserved gene with putative nucleolar functions. *Nat Genet* 1998; **19**: 32–38.
44 Mitchell JR, Wood E, Collins K. A telomerase component is defective in the human disease dyskeratosis congenita. *Nature* 1999; **402**: 551–555.
45 Sieron P, Hader C, Hatina J, Engers R, Wlazlinski A, Muller M *et al.* DKC1 overexpression associated with prostate cancer progression. *Br J Cancer* 2009; **101**: 1410–1416.
46 Montanaro L, Brigotti M, Clohessy J, Barbieri S, Ceccarelli C, Santini D *et al.* Dyskerin expression influences the level of ribosomal RNA pseudo-uridylation and telomerase RNA component in human breast cancer. *J Pathol* 2006; **210**: 10–18.
47 Montanaro L, Calienni M, Ceccarelli C, Santini D, Taffurelli M, Pileri S *et al.* Relationship between dyskerin expression and telomerase activity in human breast cancer. *Cell Oncol* 2008; **30**: 483–490.
48 Chang TC, Yu D, Lee YS, Wentzel EA, Arking DE, West KM *et al.* Widespread microRNA repression by Myc contributes to tumorigenesis. *Nat Genet* 2008; **40**: 43–50.

Supplementary Information accompanies the paper on the Leukemia website (http://www.nature.com/leu)

Jpn J Ophthalmol (2011) 55:495–501
DOI 10.1007/s10384-011-0065-8

CLINICAL INVESTIGATION

Diagnosis of ocular toxoplasmosis by two polymerase chain reaction (PCR) examinations: qualitative multiplex and quantitative real-time

Sunao Sugita · Manabu Ogawa · Shizu Inoue · Norio Shimizu · Manabu Mochizuki

Received: 26 December 2010 / Accepted: 19 April 2011 / Published online: 13 July 2011
© Japanese Ophthalmological Society 2011

Abstract
Aim To establish a two-step polymerase chain reaction (PCR) diagnostic system for ocular toxoplasmosis.
Methods A total of 13 ocular fluid samples (11 aqueous humor and 2 vitreous fluid) were collected from 13 patients with clinically suspected ocular toxoplasmosis. Ten ocular samples from other uveitis patients and 20 samples from subjects without ocular inflammation were used as controls. Two polymerase chain reaction (PCR) methods, i.e., qualitative multiplex PCR and quantitative real-time PCR, were used to measure the toxoplasma genome (*T. gondii* B1 gene).
Results Qualitative multiplex PCR detected *T. gondii* B1 gene in the ocular fluids of 11 out of 13 patients with clinically suspected ocular toxoplasmosis. In real-time PCR, we detected high copy numbers of *T. gondii* DNA (5.1×10^2–2.1×10^6 copies/mL) in a total of 10 patients (10/13, 77%). Only ocular toxoplasmosis scar lesions were observed in the three real-time PCR-negative patients. PCR assay results for the samples from the two control groups were all negative.
Conclusions The two-step PCR examination to detect toxoplasma DNA is a useful tool for diagnosing ocular toxoplasmosis.

S. Sugita (✉) · M. Ogawa · S. Inoue · M. Mochizuki
Department of Ophthalmology and Visual Science,
Tokyo Medical and Dental University Graduate
School of Medicine, 1-5-45 Yushima, Bunkyo-ku,
Tokyo 113-8519, Japan
e-mail: sunaoph@tmd.ac.jp

N. Shimizu
Department of Virology, Medical Research Institute,
Tokyo Medical and Dental University Graduate
School of Medicine and Dental Sciences, Tokyo, Japan

Keywords Ocular toxoplasmosis · Polymerase chain reaction · Uveitis · Ocular fluids

Introduction

Ocular toxoplasmosis is a sight-threatening intraocular inflammatory disorder prevalent in many parts of the world. In clinical practice, ocular toxoplasmosis diagnosis is made based on *Toxoplasma gondii* (*T. gondii*) serological tests and on the findings of typical ocular manifestations, for example old retinal necrotic lesions with pigmentation and fresh retinal lesions adjacent to chorioretinal atrophic lesions. However, there are many asymptomatic sero-positive individuals in the area in which *T. gondii* is endemic, with atypical lesions of ocular toxoplasmosis that resemble other necrotizing retinitis, for example acute retinal necrosis and cytomegalovirus retinitis. It is, therefore, necessary to perform laboratory tests to confirm toxoplasmosis infections in the eye. Ocular fluids, which include the aqueous humor and vitreous fluid, are ideal samples for this test, because they can be used to examine local specific antibody production (Goldmann–Witmer coefficient; GWC) or *T. gondii* DNA by polymerase chain reaction (PCR). Previous reports reveal that GWC and PCR assays performed on ocular samples can play a prominent role in the diagnosis of *Toxoplasma* infections [1–12]. Because local specific antibody production is often unpredictable in immunocompromised patients, the PCR assay is reported to be a better diagnostic tool [10]. In addition, the PCR assay can also be used to examine ocular samples for the purpose of diagnosing ocular toxoplasmosis in immunocompetent patients [11] and the atypical strain of *T. gondii* [12]. Moreover, previous studies found that PCR is a rapid and sensitive method